Regulation of Ferroptosis in Obesity: Muscle Type-Specific Effects of Dietary Restriction and Exercise

Fujue Ji[1, 2], Yu Jin Park[1], Haesung Lee[1, 2], and Jong-Hee Kim[1, 2, #]

[1] Major in Sport Science, Division of Sport Industry and Science, College of Performing Arts and Sport, Hanyang University, 222 Wangsimni-ro, Seongdong-gu, Seoul, Republic of Korea

[2] BK21 FOUR Human-Tech Convergence Program, Hanyang University, 222 Wangsimni-ro, Seongdong-gu, Seoul 04763, Republic of Korea

[#] Corresponding Author

carachel07@hanyang.ac.kr

Background

Obesity is a significant global health issue and a risk factor for numerous diseases. Ferroptosis, an iron-dependent regulated cell death, is triggered by iron overload and the excessive accumulation of lipid peroxidation mediated by reactive oxygen species. Studies has identified a strong association between ferroptosis and obesity. Additionally, dietary restriction (DR) and DR combined with exercise (DR+Ex) are effective strategies for managing obesity and ferroptosis. However, the regulation of ferroptosis and its signaling pathways in skeletal muscle under conditions of obesity, DR, and DR+Ex remains poorly understood.

Methods

Mice were divided into four groups: normal diet, high-fat diet, high-fat DR, and high-fat DR+Ex. All mice were fed ad libitum with either a normal or high-fat diet for the first 14 weeks, followed by the respective interventions for the subsequent 8 weeks. Mice muscle ferroptosis were examined by immunohistochemistry, Hematoxylin & Eosin, Masson's trichrome, Prussian blue staining, and Western-Immunoblot.

Results

The high-fat diet resulted in increased inflammatory cell infiltration, fibrosis, and iron accumulation. Red and white muscles showed increased expression of 4-HNE, regulated by GPX4 and NCAO4, respectively. DR and DR+Ex reduced downstream 4-HNE expression by regulating GPX4 in red muscle.

Conclusion

Red and white muscles respond to obesity-induced ferroptosis through different signaling pathways. The regulation of ferroptosis by DR and DR+Ex is muscle type-specific. Specifically, red muscle is more sensitive to the regulation of ferroptosis signaling by DR and DR+Ex compared to white muscle.

Keywords: Obesity, Ferroptosis, Muscle type-specific, Dietary restriction, Exercise

1. Introduction

Obesity has emerged as a significant global health issue, affecting millions of individuals worldwide. Its detrimental effects on human health are well-documented, with numerous studies linking it to chronic diseases such as cardiovascular disorders, type 2 diabetes, and certain types of cancer (Blüher, 2019). Recent research has found that various chronic diseases caused by obesity are related to its induction of multiple cell death pathways, including ferroptosis (Stockwell et al., 2017).

Ferroptosis is an iron-dependent form of regulated cell death caused by iron overload and the excessive accumulation of lipid peroxidation products mediated by reactive oxygen species (ROS) (Dixon et al., 2012). This unique cell death mechanism has been implicated in the pathogenesis of various diseases across different organs and tissues, including neurodegenerative disorders, liver diseases, and kidney injury (Stockwell & Jiang, 2019). Studies have found that obesity can lead to tissue or organ damage and functional decline by regulating ferroptosis. Specifically, obesity induces ferroptosis signaling, leading to varying degrees of damage and functional impairment in the heart (Pei et al., 2021), liver (Luo et al., 2020), kidneys (Luo et al., 2020),and pancreas (Wei et al., 2020).

Unexpectedly, recent studies have highlighted the close association between ferroptosis and skeletal muscle-related disorders (Wang et al., 2020; Wang et al., 2022). Ferroptosis not only induces skeletal muscle cell death but also inhibits their proliferation and differentiation (Ding et al., 2021; Guerrero-Hue et al., 2019; Huang et al., 2021). Consequently, it is strongly associated with conditions such as sarcopenia, rhabdomyolysis, rhabdomyosarcoma, and exhaustive exercise-induced fatigue (Dächert et al., 2020; Guerrero-Hue et al., 2019; Huang et al., 2021; Xiao et al., 2022). These skeletal muscle disorders significantly impair patients' quality of life and physical function, and can lead to acute and chronic diseases such as diabetes, bone fractures, hypercalcemia, and acute kidney injury (Liu et al., 2014; Oliveira & Vaz, 2015; Tsekoura et al., 2017; Welch et al., 2020). However, the regulatory effect of obesity on ferroptosis in skeletal muscle is currently unclear.

Dietary restriction (DR) has been extensively studied for its potential health benefits, including increased lifespan, improved metabolic health, and reduced risk of age-related diseases (Mattson et al., 2017). DR not only ameliorates obesity-induced skeletal muscle dysfunction (Suga et al., 2014) but also reduces the excessive accumulation of ROS (Bevilacqua et al., 2005; Walsh et al., 2014). ROS causes lipid peroxidation, ultimately leading to ferroptosis by reacting with polyunsaturated fatty acids in phospholipid membranes (Han et al., 2020; Li et al., 2020). The inhibitory effect of DR on obesity and lipid peroxidation may be a potential mechanism to regulate the ferroptosis signaling pathway in skeletal muscle. Exercise (Ex) is widely recognized for its positive impact on health (Ruegsegger & Booth, 2018). Ex not only improves obesity- and ROS-induced skeletal muscle dysfunction (Ostler et al., 2014) but also modulates the expression of ferroptosis signaling in the brain, kidney, and nerves (Chen et al., 2023; Liu et al., 2022; Xiang et al., 2023). Dietary restriction combined with exercise (DR+Ex) is acknowledged as a method that more effectively counteracts the negative effects of obesity and lipid peroxidation than DR or Ex alone (Khachatoorian & Samara, 2018; Kim et al., 1996; Kvedaras et al., 2020; Li et al., 2017). However, the regulatory effects of DR and DR+Ex on obesity-induced ferroptosis in skeletal muscle remain unclear.

Given the critical role of skeletal muscle in overall health and the emerging evidence linking

ferroptosis to muscle disorders, it is imperative to investigate the regulation of ferroptosis in the context of obesity, DR, and DR+Ex. Understanding the molecular mechanisms underlying these processes could provide valuable insights into the development of targeted interventions for obesity-related muscle disorders and promote overall health and well-being.

2. Methods

2.1 Animals and Experimental Design

Male C57BL/6N mice (14 months old) were randomly divided into four experimental groups: Normal diet (ND, n=7), High-fat diet (HF, n=7), 20% high-fat dietary restriction (HFR, n=7), and 20% high-fat dietary restriction with voluntary wheel running exercise (HFRV, n=7). For the first 4 months, all mice were fed either a standard chow diet (ND; Teklad Global 2018, Envigo Inc.) or a high-fat diet (HF; 45% kcal from fat, D12451, Research Diets Inc.). In the subsequent 4 months, dietary restriction (DR) and dietary restriction combined with exercise (DR+Ex) interventions were applied to the respective groups (Figure 1). The mice were housed in a controlled environment, maintained at a temperature of 22 ± 2 °C with 50–60% humidity, and subjected to a 12-hour light/dark cycle. All animals had ad libitum access to water and were allowed physical activity. The experimental procedures were approved by the Institutional Animal Care and Use Committee (IACUC) of Hanyang University (HYU 2021-0239A).

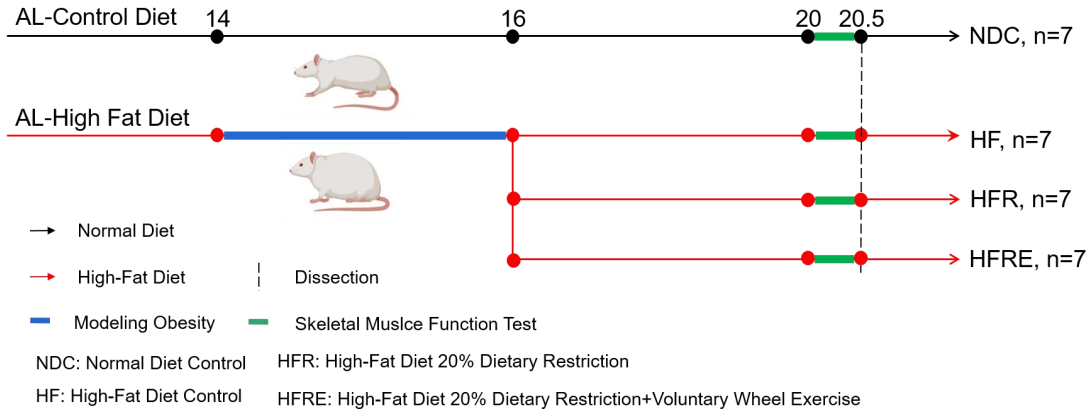

Figure 1. Schematic overview experimental study design..

2.2 Body Composition

Mice were anesthetized with 40 mg/kg ketamine and 0.8 mg/kg medetomidine and analyzed for body composition using an InAlyzer Dual-energy X-ray Absorptiometry (DEXA) system (Micro Photonics Inc., PA, USA). The parameters measured included total mass (g), lean mass ratio (%), fat mass (g), lean mass (g), fat content in tissue (%), and fat mass ratio (%).

2.3 Skeletal Muscle Function Tests

All mice underwent skeletal muscle function tests before euthanasia. Skeletal muscle function was assessed in four groups of mice using tests for walking speed, endurance, physical activity, and grip strength (Figure 1).

Rota-Rod test: Walking speed was assessed using the Rota-Rod test (Leem et al., 2022). An adaptation period was conducted during the first three days, involving a pre-test exercise at 5 rpm for 1 minute, once per day. The official test utilized an acceleration mode, where the speed

increased from 5 to 50 rpm over a 5-minute period (Model 76-0770, Harvard Apparatus Inc., Holliston, MA, USA). The latency to fall from the device was recorded. Each mouse was tested three times with a ten-minute interval between tests, and the best performance out of the three trials was used as the outcome measure.

Treadmill test: Endurance capacity was evaluated using a treadmill test (Alghannam et al., 2016). Adaptation was performed three days before the official test, consisting of running at 5 cm/s for 5 minutes, once per day, on a 0-degree slope. During the official test, the treadmill speed increased by 1 cm/s every 20 seconds starting from 5 cm/s, with a 0-degree slope. The trial ended when the mouse touched the shock pad (set at 0.6 mA) three times.

Voluntary wheel test: Physical activity was measured using the voluntary wheel test (Manzanares et al., 2018). Running distance was recorded using a voluntary wheel (MAN86130, Lafayette Instrument Company, Lafayette, IN, USA), with each wheel rotation corresponding to a distance of 0.4 m. The average running distance over a 5-day period was recorded for each mouse.

Inverted-cling grip test: Grip strength was assessed using the inverted-cling grip test (Graber et al., 2013). Adaptation was conducted prior to the official test, with the adaptive test performed once a day for three days. During the official test, mice were placed in the center of a wire mesh screen, and a stopwatch was started. The screen was then rotated to an inverted position over 2 seconds, with the mouse's head descending first, and held 40-50 cm above a padded surface. The time until the mouse fell was recorded. This measurement was repeated three times with ten-minute intervals between tests, and the maximum reading was recorded.

2.4 Preservation and Preparation of Skeletal Muscle

The anesthetized mice were euthanized by cervical dislocation. Following euthanasia, the gastrocnemius (GAS) muscles were carefully dissected from the mice. The left leg muscles were fixed in 10% formalin for 24 hours, then dehydrated and embedded in paraffin. Sections were prepared for Hematoxylin and Eosin (H&E) staining, Prussian blue staining, Masson's trichrome staining, and immunohistochemistry (IHC). The right leg muscles were snap-frozen in liquid nitrogen and stored at –80°C for subsequent Western-immunoblot (WB) analyses.

2.5 Hematoxylin and Eosin (H&E) staining

Rehydrated tissue sections (5 μm) were stained using ClearView™ hematoxylin (MA0101010, StatLab, McKinney, TX, USA) for 2-3 minutes, rinsed in tap water for 30-60 seconds, differentiated in 1% hydrochloric acid alcohol for 5-10 seconds, washed in tap water for 3-5 minutes, and stained with ClearView™ eosin (MA0101015, StatLab, McKinney, TX, USA) for 1-2 minute. Subsequently, the sections were dehydrated, cleared, and mounted with neutral resin. Images were acquired using a slide scanner (Axio Scan. Z1, Zeiss) at 200x magnification. For each mouse, a single section of each skeletal muscle was randomly photographed to obtain 5 images, each covering an area of 0.271 square millimeters. The average of these five images was used to represent the cross-sectional area (CSA) of that skeletal muscle for the mouse. The CSA of each muscle fiber was automatically analyzed using “Cellpose,” an open-source deep learning-based segmentation tool (Stringer et al., 2021).

2.6 Prussian Blue Staining

After deparaffinization and rehydration, the paraffin tissue sections (5 μm) were stained using

150 Prussian Blue staining kit (G1422, Beijing Solarbio Science & Technology Co., Ltd.). Images
151 were acquired using a slide scanner (Axio Scan. Z1, Zeiss) at 200x magnification. For each mouse,
152 a single section of each skeletal muscle was randomly photographed to obtain 5 images, each
153 covering an area of 0.271 square millimeters. The average of these five images was used to
154 represent the value of that iron accumulation for the mouse. ImageJ software was used for the
155 analysis.

156 ***2.7 Masson's Trichrome Staining***

157 After deparaffinization and rehydration, the paraffin tissue sections (5 μm) were stained using
158 Masson's trichrome staining kit (G1340, Beijing Solarbio Science & Technology Co., Ltd.).
159 Images were acquired using a slide scanner (Axio Scan. Z1, Zeiss) at 200x magnification. For
160 each mouse, a single section of each skeletal muscle was randomly photographed to obtain 5
161 images, each covering an area of 0.271 square millimeters. The average of these five images was
162 used to represent the ECM value of that skeletal muscle for the mouse. ImageJ software was used
163 for analysis. A threshold was established to remove the blank background, the ECM signal was
164 isolated using color deconvolution and thresholding, and the area of the ECM signal was
165 subsequently compared with the net area of the muscle section using ImageJ software.

166 ***2.8 Western-Immunoblot (WB)***

167 The red and white GAS were dissected separately (Chen et al., 2015). The muscles were lysed
168 using an EzRIPA Lysis Kit (WSE-7420, ATTO). Protein concentration was determined using the
169 Pierce™ Bicinchoninic Acid Protein Assay Kit (Thermo Scientific, Waltham, MA, USA). Equal
170 amounts of protein samples (40 μg) were separated by sodium dodecyl sulfate-polyacrylamide gel
171 electrophoresis and electro-transferred to nitrocellulose membranes (Bio-Rad Laboratories,
172 Hercules, CA, USA). The membranes were blocked with 5% non-fat milk dissolved in
173 Tris-buffered saline with Tween-20 (TBST; 10 mM Tris, 150 mM NaCl, and 0.1% Tween-20; pH
174 7.6) for 1.5 hours at room temperature and then incubated with primary antibodies (Table 1)
175 overnight at 4°C. Subsequently, the membranes were incubated with horseradish
176 peroxidase-conjugated secondary antibodies (Table 1) for 1.5 hours at room temperature. The
177 targeted bands were quantified by densitometry using ImageJ software.

178 ***2.9 Immunohistochemistry (IHC)***

179 Following the immunohistochemistry protocol with modifications based on Magaki et al.,
180 paraffin-embedded tissue sections (5 μm) were deparaffinized and rehydrated (Magaki et al.,
181 2019). Heat-induced antigen retrieval was performed using 0.01 mol/L sodium citrate buffer (pH
182 6.0, C1010, Beijing Solarbio Science & Technology Co., Ltd.) in a microwave oven for 20
183 minutes at 100°C. The sections were then washed twice with Phosphate-buffered saline (PBS;
184 0.137M NaCl, 0.0027M KCL, 0.010mM Na_2HPO_4, and 0.002mM KH_2PO_4; pH 7.2) for 5 minutes
185 each and blocked with 3% hydrogen peroxide (4104-4400, DAE JUNG) for 15 minutes twice to
186 remove endogenous peroxidases. Following three additional 5-minute washes with PBS, the
187 sections were blocked with 100-200 μl of blocking buffer (5% Bovine serum albumin in PBS) for
188 30 minutes at room temperature. After blocking, the sections were washed three times with PBS
189 for 5 minutes each and incubated with the primary antibody (Table 1) overnight at 4°C. The
190 sections were then washed three times with PBS for 5 minutes each and incubated with the

secondary antibody (Table 1) in a humidified chamber for 60 minutes at room temperature. Following three more 5-minute washes with PBS, the sections were incubated with the Pierce™ DAB Substrate Kit (Thermo Scientific, #34002) for 6 minutes and washed three times with PBS for 5 minutes each. Finally, the sections were rehydrated and mounted. Images were acquired using a slide scanner (Axio Scan. Z1, Zeiss) at 200x magnification. For each mouse, a single section of each skeletal muscle was randomly photographed to obtain 5 images, each covering an area of 0.271 square millimeters. The average of these five images was used to represent the antibody expression value of that skeletal muscle for the mouse. ImageJ software was used for analysis.

Table 1. Primary and secondary antibodies.

Antibodies	Source	Vender	Catalog	Dilution (WB)	Dilution (IHC)
P53	Rabbit	Cell signaling	#30313	1:500	
SLC7A11	Rabbit	Abcam	ab175186	1:1000	
GAPDH	Rabbit	Cell signaling	#5174	1:3000	
GPX4	Rabbit	Abcam	ab125066	1:1000	
AMPK	Rabbit	Cell signaling	#5831	1:500	
p-AMPK	Rabbit	Cell signaling	#2535	1:500	
TFR1	Rabbit	Abcam	ab84036	1:500	
NCOA4	Rabbit	Invitrogen	#PA5-115626	1:500	
4-HNE	Rabbit	Abcam	ab46545	1:1000	1:200
MDA	Mouse	Abcam	ab243066	1:250	1:100
Adiponectin	Rabbit	Cell signaling	#2789	1:1000	
Leptin	Rabbit	Invitrogen	PA1-052	1:500	
Goat anti Rabbit	Goat	Invitrogen	#G-21234	1:5000	1:500
m-IgG Fc	-	SANTA	sc-525409	1:5000	1:25

2.10 Statistical Analysis

Statistical analyses were performed using GraphPad Prism software (version 9). Comparisons between two groups were conducted using an unpaired Student's t-test. For comparisons among three groups, a one-way analysis of variance (ANOVA) followed by a least significant difference (LSD) post-hoc test was employed. To assess the effects of muscle type (white vs. red) and dietary conditions (HF vs. DR vs. DR+Ex), a two-way ANOVA with Bonferroni's post-hoc test was applied. Outliers were identified and removed using the Z-score approach prior to conducting statistical analyses to ensure the robustness and reliability of the results. All results are expressed as the mean ± standard deviation (SD). Statistical significance was set at $p < 0.05$, with asterisks indicating the following levels of significance: *$p < 0.05$, **$p < 0.01$, ***$p < 0.001$, and ****$p < 0.0001$.

3. Results

3.1 High-Fat Diet-Induced Obesity Evokes Dysfunction and Ferroptosis in Skeletal Muscle

To investigate whether obesity regulates ferroptosis in skeletal muscle, we induced obesity in mice by feeding them a high-fat diet for 14 weeks. All the data are shown in Figure 2.

DEXA analysis revealed that high-fat diet intake led to increases in body weight ($P < 0.0001$), lean

mass (P = 0.0021), fat mass (P < 0.0001), fat mass ratio (P < 0.0001), and fat mass in tissues (P < 0.0001), while the lean mass ratio decreased (P < 0.0001) (Figure 2A-H). These indicators are widely used to evaluate and identify mouse models of obesity (Chen et al., 2012; Koza et al., 2006; Y. Yang et al., 2014; Yeu et al., 2019). Consistent with impaired skeletal muscle function in obese mice (Graham et al., 2019; Vellers et al., 2017), we found that a high-fat diet significantly reduced walking speed (P = 0.0424), grip strength (P = 0.0053), and endurance in mice (P = 0.0217) (Figure 2I-K). These findings further validate the successful establishment of the obese mouse model.

Histological features of ferroptosis include the accumulation of inflammatory cells in organs and tissues (Zhang et al., 2023) and fibrosis (Yu et al., 2020). H&E staining revealed that although the CSA of HF skeletal muscle significantly increased (P = 0.00210), it was accompanied by substantial inflammatory cell infiltration (Figure 2M and O). Additionally, Masson's trichrome staining indicated a significant increase in skeletal muscle fibrosis in HF compared to NDC (P = 0.0110) (Figure 2N and P). Ferroptosis is highly associated with lipid peroxidation and abnormal iron accumulation (Dixon et al., 2012). As products of lipid peroxidation, malondialdehyde (MDA) and 4-hydroxynonenal (4-HNE) can reflect the extent of ferroptosis in cells (Chen et al., 2021; Tang et al., 2021). IHC analysis showed elevated levels of lipid peroxidation products 4-HNE (P = 0.0320) and MDA (P = 0.0150) in HF skeletal muscle compared to NDC (Figure 2Q-S). Furthermore, Prussian blue staining revealed abnormal iron accumulation in HF skeletal muscle (P = 0.0210) (Figure 2T-V). These data indicate that high-fat diet induces obesity, leading to skeletal muscle dysfunction and ferroptosis in mice.

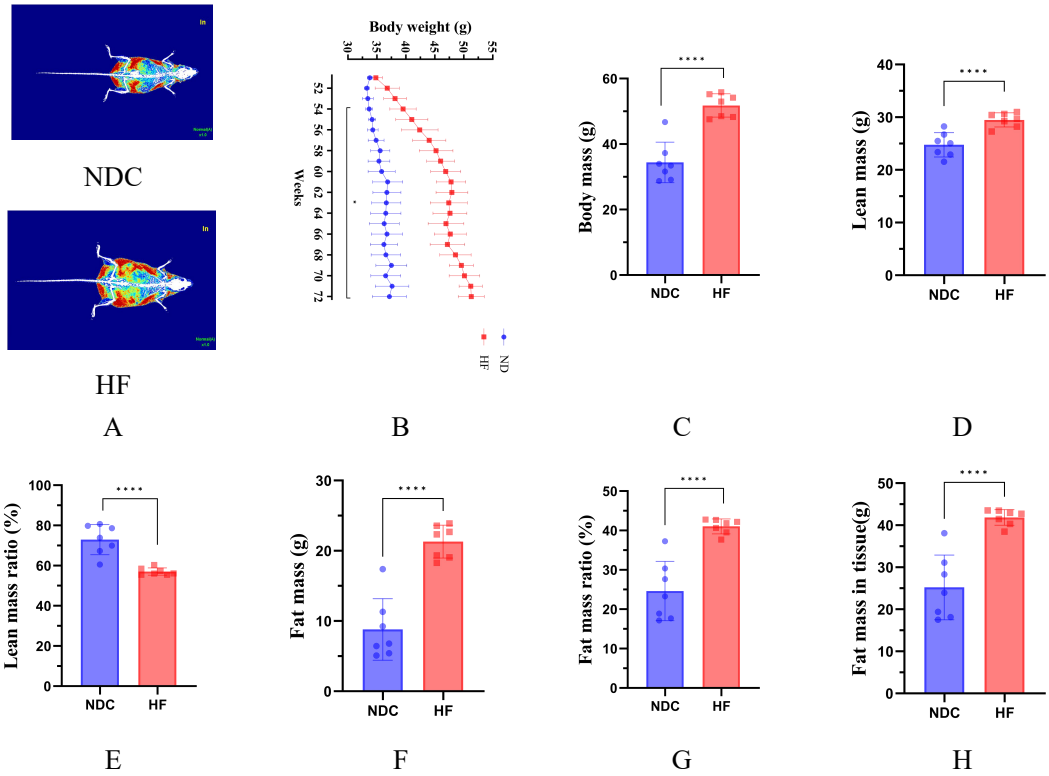

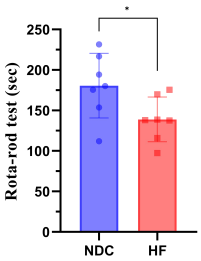

I

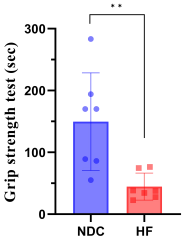

J

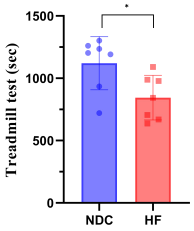

K

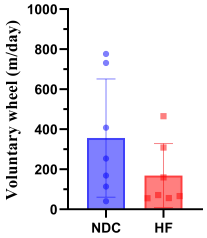

L

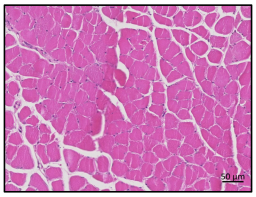

NDC

NDC

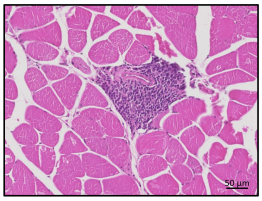

HF

H&E Staining

M

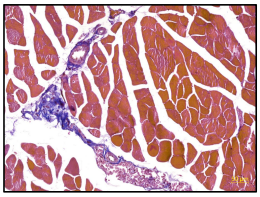

HF

Masson Staining

N

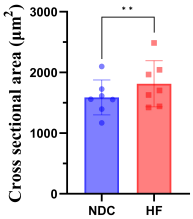

O

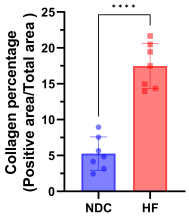

P

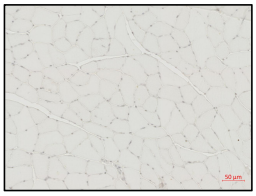

IHC: Negative control

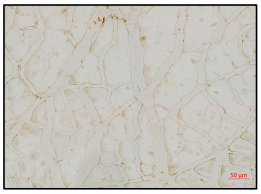

NDC

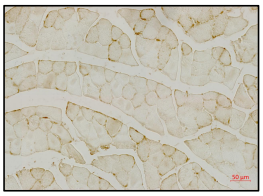

HF

IHC: 4-HNE

Q

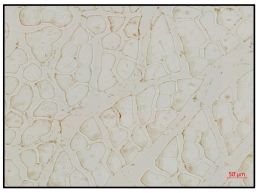

NDC

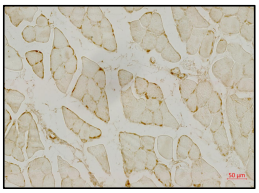

HF

IHC: MDA

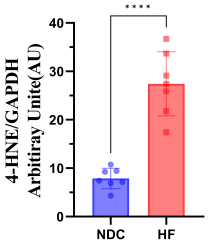

R

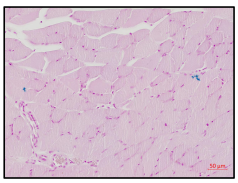

NDC

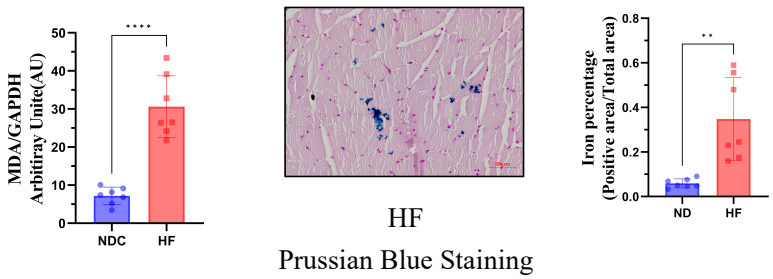

S T U

Figure 2. High-fat diet-induced obesity evokes dysfunction and ferroptosis in skeletal muscle. (A) Representative DEXA-scanned images of NDC and HF mice; skeletal muscle, fat tissue, and bone are shown in blue, red, and white, respectively. (B) Weekly body weight changes (group × weeks): NDC vs. HF (, 54-72 weeks). (C-H) Quantitative data of final total mass, lean mass, lean mass ratio, fat mass, fat mass ratio, and fat mass in tissue, respectively, were acquired by DEXA scanning. (I-L) Skeletal muscle function tests: (I) Walking speed test. (J) Strength test. (K) Endurance test. (L) Physical activity test. (M-N) Representative images showing H&E staining and Masson's trichrome staining of gastrocnemius. The collagen is indicated in blue and the muscle in red. (O) Skeletal muscle cross-sectional area in NDC and HF. (P) Skeletal muscle collagen area in NDC and HF. (Q) Representative images of IHC. (R) 4-HNE expression levels in skeletal muscle. (S) MDA expression levels in skeletal muscle. (T) Representative images of Prussian blue staining. The iron is indicated in blue and the muscle in red. (U) Iron percentage in skeletal muscle. Significant differences are denoted by asterisks: $p < 0.05$ (*), $p < 0.01$ (**), $p < 0.001$ (***), and $p < 0.0001$ (****). All values are presented as mean ± SD. Normal diet (ND, n=7), high-fat diet (HF, n=7). Scale bar = 50 µm.*

3.2 Muscle Type-Specific Regulation of Ferroptosis by GPX4 and NCOA4 in High-Fat Diet-Induced Obesity.

Given the observed ferroptosis in skeletal muscle as a result of obesity, we employed WB analysis to investigate the impact of obesity on the expression of representative proteins in five ferroptosis-related signaling pathways: amino acid metabolism, lipid metabolism, iron metabolism, lipophagy, and ferritinophagy in different muscle types. All the data are shown in Figure 3.

Under normal diet conditions, the expression of Glutathione peroxidase 4 (GPX4) (P = 0.0073) and Nuclear receptor coactivator 4 (NCOA4) (P = 0.0007) was significantly higher, and 4-HNE (P = 0.002) was lower in white muscle compared to red muscle (Figure 3A and H). Under high-fat diet conditions, the expression of NCOA4 was significantly lower in white muscle compared to red muscle (P < 0.0001) (Figure 3G). Additionally, within the same muscle type, a high-fat diet significantly decreased the expression of GPX4 (P = 0.0007) and NCOA4 (P = 0.0015) and increased 4-HNE (P < 0.0001) in white muscle compared to a normal diet (P < 0.05) (Figure 3A, G, and H). Although a high-fat diet did not alter the expression of GPX4 in red muscle, it significantly increased the expression of NCOA4 (P < 0.0001) and 4-HNE (P = 0.0375) (Figure 3A, G, and H). These data show muscle type-specific regulation of ferroptosis by GPX4 and NCOA4 in high-fat diet-induced obese mice. Specifically, obesity regulates ferroptosis by decreasing the expression of GPX4 in white muscle and increasing the expression of NCOA4 in red muscle.

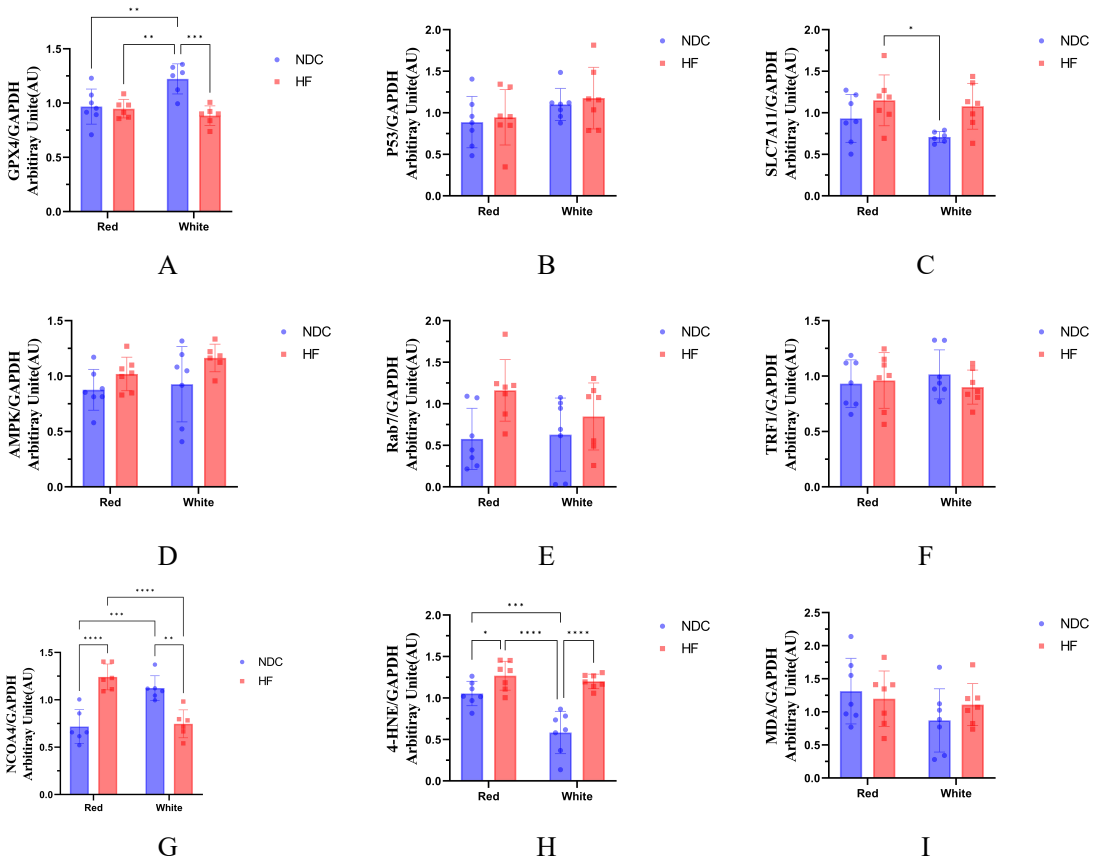

Figure 4. Muscle type-specific regulation of ferroptosis by GPX4 and NOCA4 in high-fat diet-induced obese mice. WB was performed for protein expression levels of ferroptosis signaling pathways, (A): Glutathione peroxidase 4 (GPX4), (B): P53, (C): Solute Carrier Family 7 Member 11 (SLC7A11), (D): AMP-activated protein kinase (AMPK), (E): Ras-related protein Rab-7a (Rab7), (F): Telomeric repeat-binding factor 1 (TRF1), (G) Nuclear Receptor Coactivator 4 (NCOA4), (H): 4-Hydroxynonenal (4-HNE), and (I): Malonaldehyde (MDA). Significant differences are denoted by asterisks: $p < 0.05$ (*), $p < 0.01$ (**), $p < 0.001$ (***) and $p < 0.0001$ (****). All values are presented as mean ± SD. Normal diet (ND, n=7), High-fat diet (HF, n=7).

3.3 DR and DR+Ex Show Some Improvements and Regulation in Body Composition and Ferroptosis in Obese Mice.

Previous studies have extensively reported the positive effects of DR and DR+Ex on obesity, lipid peroxidation, ROS, and even ferroptosis (Bevilacqua et al., 2005; Chen et al., 2023; Li et al., 2017; Liu et al., 2022; Walsh et al., 2014). Therefore, we investigated the effects of DR and DR+Ex intervention on ferroptosis in the skeletal muscle of high-fat diet-induced obese mice. All the data are shown in Figure 4.

Results showed significant differences in body weight between the HF and HFRV groups at 70 weeks (P = 0.0435) (Figure 4B). Compared to the HF, HFRV significantly reduced total mass (P = 0.0061), lean mass (P = 0.0171), and fat mass in mice (P = 0.0159), but there were no changes in lean mass ratio, fat mass ratio, or fat mass in tissues (Figure 4C-H). DR and DR+Ex did not appear to effectively improve skeletal muscle function in high-fat diet-induced obese mice (Figure 4I-L).

Additionally, H&E staining showed that DR and DR+Ex reduced inflammatory cell infiltration in muscle fibers; however, DR+Ex also decreased the CSA of skeletal muscle (P = 0.0296) (Figure

4M and O). Masson's trichrome staining and Prussian blue staining indicated fibrosis and iron in skeletal muscle were not significant changes (Figure 4N, P, T, and U). Lastly, IHC analysis showed no significant differences in the expression of 4-HNE and MDA among the HF, HFR, and HFRV groups (Figure 4Q-S). These data suggest that intervention of DR and DR+Ex has limited effects on improving and regulating body composition and ferroptosis in high-fat diet-induced obese mice.

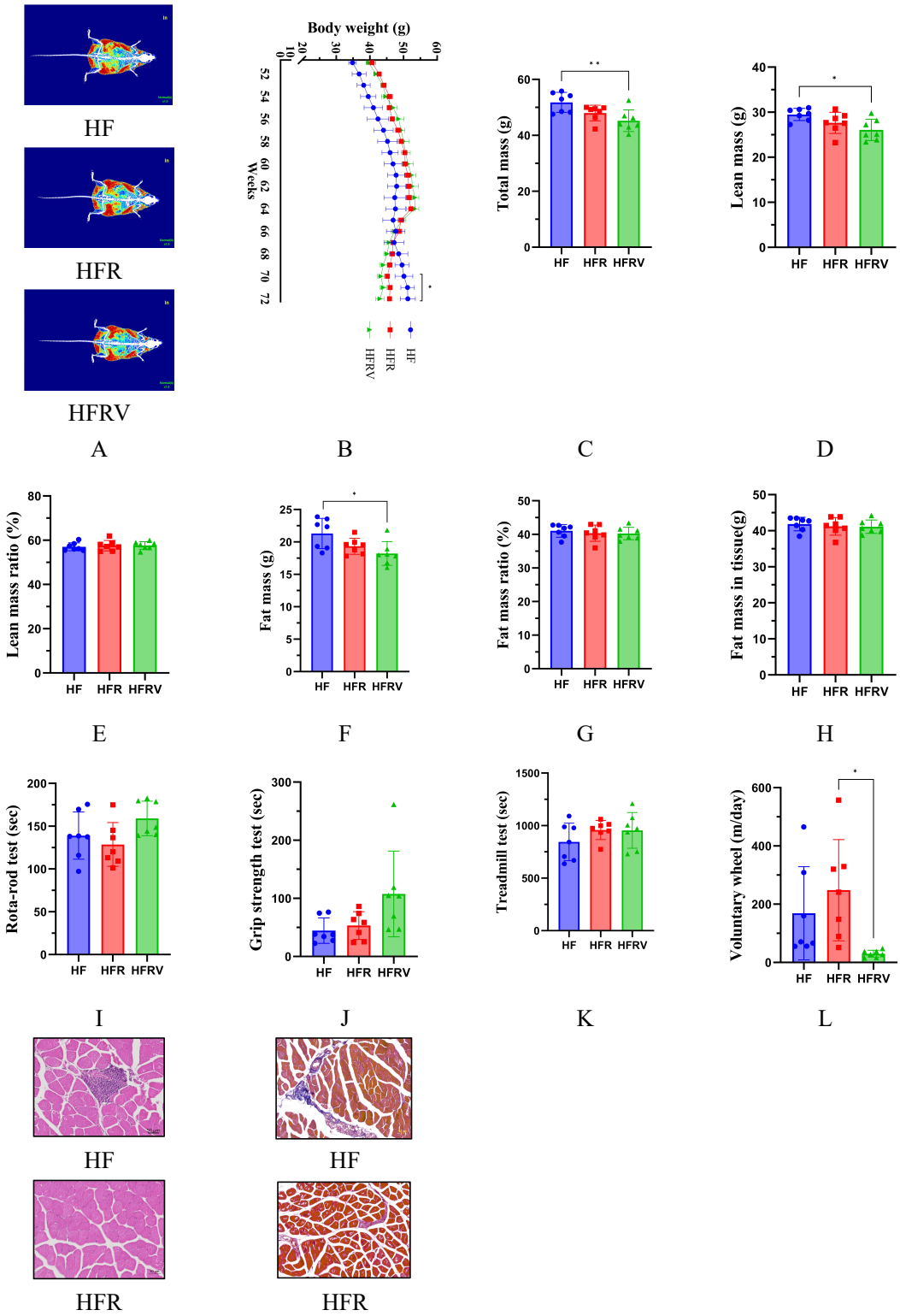

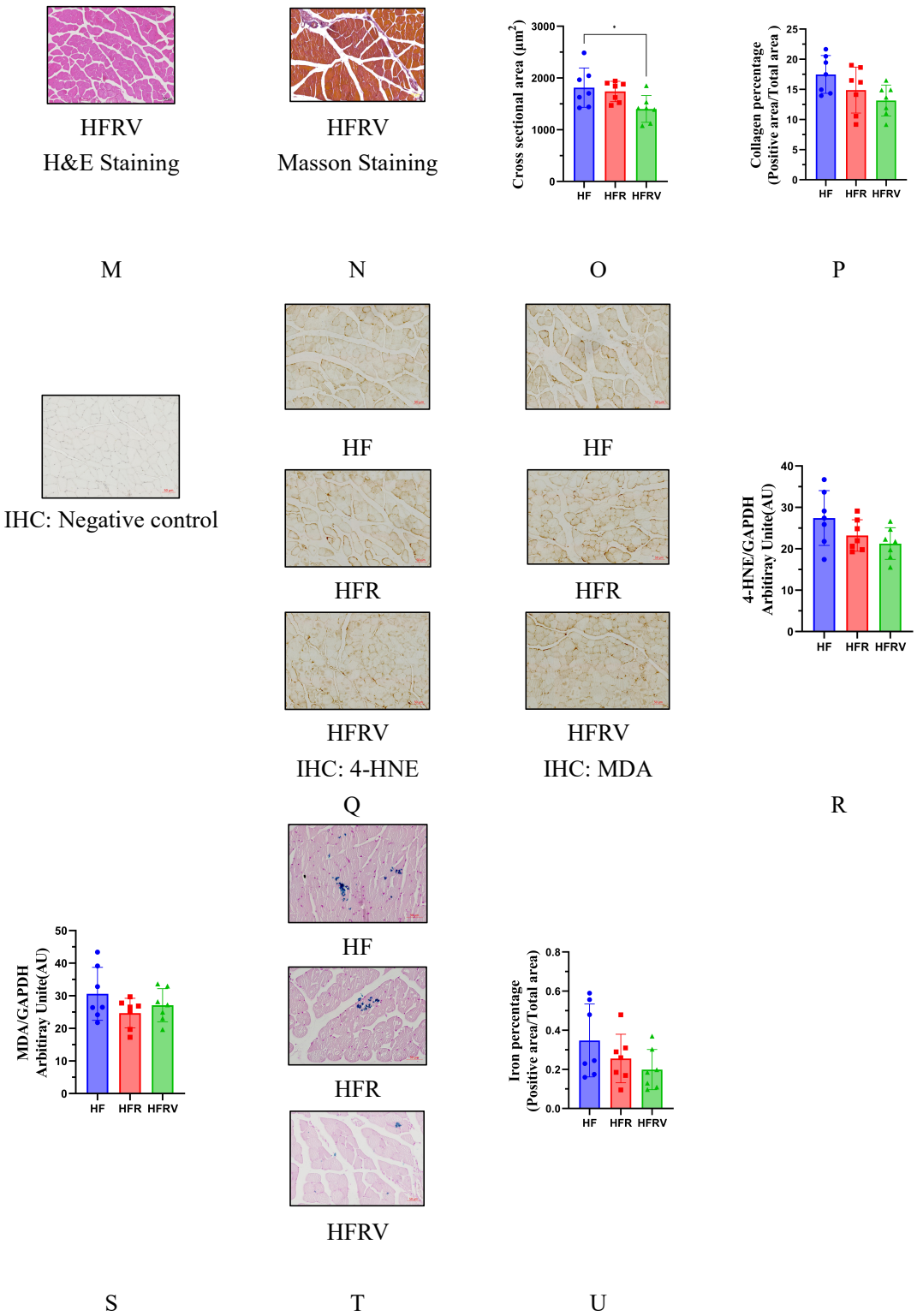

Figure 4. CR and CR+Ex were show some improvements and regulation in dysfunction and ferroptosis in skeletal muscle of high-fat diet-induced obese mice. (A) Representative DEXA-scanned images of HF, HFR, and HFRV mice; skeletal muscle, fat tissue, and bone are shown in blue, red, and white, respectively. (B) Weekly body weight changes (group × weeks): HF vs. HFRV (, 70-72 weeks). (C-H) Quantitative data of final total mass, lean mass, lean mass ratio, fat mass, fat mass ratio, and fat mass in tissue, respectively, were acquired by DEXA scanning. (I-L) Skeletal muscle function tests, (I): Walking speed test. (J): Skeletal muscle strength test. (K): Skeletal muscle endurance test. (L): Physical activity test. (M-N) Representative images showing H&E staining and Masson's*

trichrome staining of gastrocnemius. The collagen is indicated in blue and the muscle in red. (O) Skeletal muscle cross-sectional area in HF, HFR, and HFRV. (P) Skeletal muscle collagen area in HF, HFR, and HFRV. (Q) Representative images of IHC. (R) 4-HNE expression levels in skeletal muscle. (S) MDA expression levels in skeletal muscle. (T) Representative images of Prussian blue staining. The iron is indicated in blue and the muscle in red. (U) Iron percentage in skeletal muscle. Significant differences are denoted by asterisks: $p < 0.05$ (*), $p < 0.01$ (**), $p < 0.001$ (***) and $p < 0.0001$ (****). All values are presented as mean ± SD. High-fat diet (HF, n=7), 20% high-fat diet dietary restriction (HFR, n=7), and 20% high-fat diet dietary restriction + voluntary wheel running exercise (HFRV, n=7). Scale bar=50 μm.

3.4 Muscle Type-Specific Regulation of Ferroptosis by GPX4 Through DR and DR+Ex in High-Fat Diet-Induced Obese Mice

CR and CR+Ex have regulatory effects on ferroptosis in the skeletal muscle of high-fat diet-induced obese mice. However, the detailed regulatory effects on muscle type-specific ferroptosis are not well understood. Therefore, it is worthwhile to further explore the muscle type-specific regulation of ferroptosis by these interventions through different pathways. The results of the WB analysis are shown in Figure 5.

Under the same conditions (HFRV), the expression of 4-HNE in white muscle was significantly higher compared to red muscle ($P < 0.0001$) (Figure 5H). In red muscle, the expression of GPX4 was significantly higher in the HFRV group compared to the HF group ($P = 0.0471$) (Figure 5A); the expression of 4-HNE decreased sequentially in the HF, HFR, and HFRV groups, with significant differences ($P < 0.0001$ and $P = 0.0136$) (Figure 5H). In white muscle, the expression of AMP-activated protein kinase (AMPK) was significantly lower in the HFRV group compared to the HF ($P = 0.0086$) and HFR ($P = 0.0126$) groups (Figure 5D), and there were significant differences in the expression of 4-HNE between the HFR and HFRV groups ($P = 0.0427$) (Figure 5H). These data suggest that the regulation of ferroptosis by DR and DR+Ex intervention in high-fat diet-induced obese mice is muscle type-specific. Specifically, DR+Ex inhibits obesity-induced skeletal muscle ferroptosis by increasing the expression of GPX4 in red muscle.

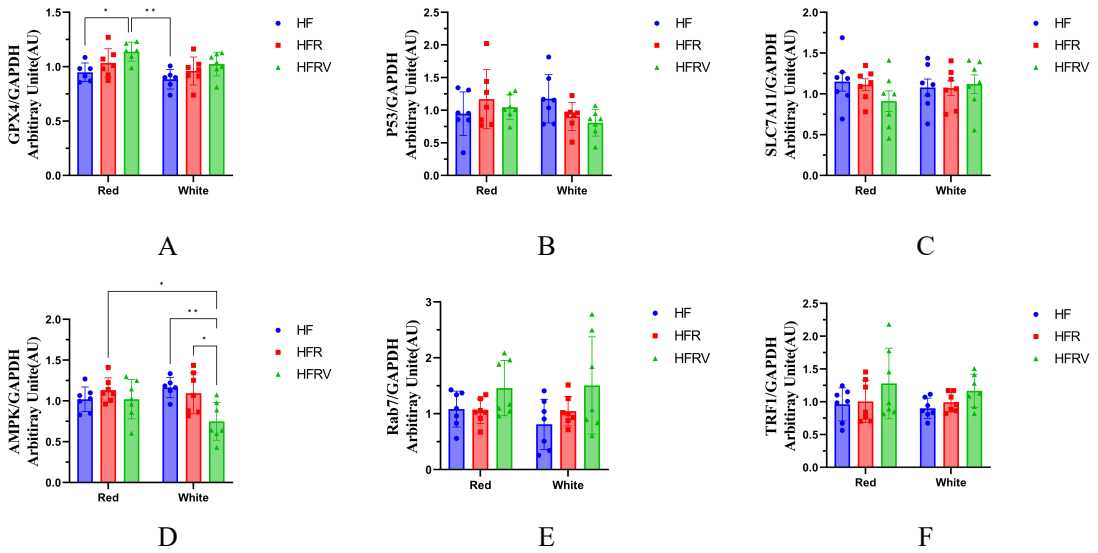

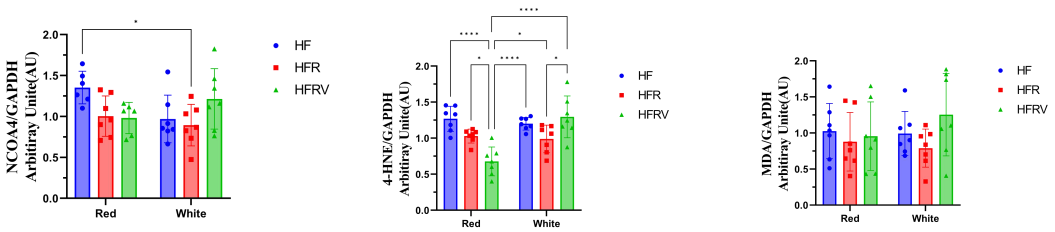

G H I

Figure 6. Through CR and CR+Ex muscle type-specific regulation of ferroptosis by GPX4 in high-fat diet-induced obese mice. WB was performed for protein expression levels of ferroptosis signaling pathways, (A): Glutathione peroxidase 4 (GPX4), (B): P53, (C): Solute Carrier Family 7 Member 11 (SLC7A11), (D): AMP-activated protein kinase (AMPK), (E): Ras-related protein Rab-7a (Rab7), (F): Telomeric repeat-binding factor 1 (TRF1), (G) Nuclear Receptor Coactivator 4 (NCOA4), (H): 4-Hydroxynonenal (4-HNE), and (I): Malonaldehyde (MDA). Significant differences are denoted by asterisks: $p < 0.05$ (*), $p < 0.01$ (**), $p < 0.001$ (***) and $p < 0.0001$ (****). All values are presented as mean ± SD. High-fat diet (HF, n=7), 20% high-fat diet dietary restriction (HFR, n=7), and 20% high-fat diet dietary restriction + voluntary wheel running exercise (HFRV, n=7).

4. Discussion

In recent years, the issue of dysfunction in cells, tissues, and organs caused by obesity has garnered widespread attention. Obesity-induced ferroptosis is considered one of the primary causes of these dysfunctions (Ganz, 2012; Ma et al., 2017; Orr et al., 2014; Zhao et al., 2022). Understanding the regulatory mechanisms of ferroptosis in the context of obesity is of significant clinical importance for related diseases. This study investigated the impact of obesity on ferroptosis in specific skeletal muscle types and the response mechanisms of its signaling pathways to DR and DR+Ex. Our research found that obesity can induce ferroptosis in skeletal muscle, while DR and DR+Ex can regulate this process. More importantly, the regulation of ferroptosis by obesity and its response to intervention are muscle type-specific. These findings enhance our understanding of the mechanisms of obesity and ferroptosis, providing a scientific basis for further in-depth studies of these diseases and cell death mechanisms.

4.1 Appropriateness of an Obesity Mouse Model.

Mice at 14 months of age are approximately equivalent to humans aged 35-45 years (Justice et al., 2016). During human aging, the prevalence of obesity increases with age. Research has shown that after the age of 40, the prevalence of obesity significantly increases (Chooi et al., 2019). In our study, mice began a high-fat diet at 14 months to simulate continuous obesity starting around age 40 in humans. We induced an obese mouse model through 4 months of a high-fat diet (D12451, Research Diets Inc.). This diet has been widely used in the construction of obese mouse models (Armani et al., 2014; Han et al., 2006; Yongbin Yang et al., 2014). Although there is no precise definition for high-fat diet-induced obese mouse models, the vast majority of studies use at least 8 weeks of ad libitum high-fat diet to create obese mouse models (Buettner et al., 2007; Han et al., 2006; Hariri & Thibault, 2010).

Additionally, after analyzing the body composition of the mice using DEXA, we found significant increases in body weight, lean mass, fat mass, fat mass in tissues, and fat mass percentage following the high-fat diet. These changes in body composition are consistent with the characteristics of obese mice reported in previous studies (Lin et al., 1977; Mandarim-de-Lacerda

et al., 2021; Rogers & Webb, 1980). Moreover, obesity leads to a decline in certain skeletal muscle functions, which is also in line with prior research, indicating that dysfunctional skeletal muscle is a hallmark of obesity (Shortreed et al., 2009; Zhang et al., 2015). Therefore, we conclude that a 4-month high-fat diet can successfully induce obesity, providing an experimental animal model for subsequent study.

4.2 High-Fat Diet-Induced Obesity Evokes Ferroptosis in Mouse Skeletal Muscle

Through H&E staining, we found that high-fat diet-induced obesity leads to inflammatory cell infiltration in skeletal muscle. In the obese state, the high expression levels of pro-inflammatory cytokines, such as TNF-α, IL-6, and IL-1β, are primarily secreted by increased infiltrating inflammatory cells (Hotamisligil, 2006; Weisberg et al., 2003). These findings are consistent with what we observed in the skeletal muscles of high-fat diet-induced obese mice.

Recent studies suggest that not only obesity but also inflammatory cell infiltration is a hallmark of ferroptosis. Ferroptosis causes lipid peroxidation of cell membranes and cell rupture, and the release of cellular contents (such as high-mobility group protein B1) can activate a local inflammatory response, leading to inflammatory cell infiltration. For instance, research by Friedmann Angeli et al. (Friedmann Angeli et al., 2014) demonstrated that ferroptosis leads to acute renal failure, accompanied by significant inflammatory cell infiltration. In the liver, where ferroptosis occurs, inflammatory cell infiltration is also present, as shown in the hemochromatosis mouse model study by Wang et al. (Wang et al., 2017). Inflammation not only hallmark of ferroptosis but also promotes it.

Oxidative stress and iron metabolism disorders in the inflammatory response can exacerbate ferroptosis, while oxidized lipid products released during ferroptosis can further promote inflammation. The study by Dixon et al. (Dixon et al., 2012) pointed out the potential inflammatory role of ferroptosis in various diseases. These research findings strongly support that ferroptosis is accompanied by inflammatory cell infiltration. In summary, ferroptosis can induce a local inflammatory response by releasing cellular contents, while inflammatory cell infiltration can exacerbate ferroptosis, forming a vicious cycle. This interaction has important pathological significance in various diseases, and further understanding of this mechanism will help develop new therapeutic strategies.

Masson's trichrome staining revealed that high-fat diet-induced obesity exacerbates skeletal muscle fibrosis. In the obese state, increased levels of oxidative stress in skeletal muscle induce oxidative damage in muscle cells, activate fibroblasts, and promote fibrosis (Furukawa et al., 2004). Inflammatory factors and oxidative stress induced by obesity not only cause damage to muscle cells but also activate fibroblasts in muscle tissue. These activated fibroblasts secrete large amounts of extracellular matrix components (ECM), such as collagen, leading to increased muscle fibrosis (Lieber & Ward, 2013). These findings are consistent with what we observed in the skeletal muscles of high-fat diet-induced obese mice.

Recently, the relationship between ferroptosis and tissue organ fibrosis has been explored in several studies. Ferroptosis, an iron-dependent form of cell death, releases oxidized lipids and cellular contents that can activate fibroblast proliferation, thereby promoting fibrosis. Specifically, cellular contents released during ferroptosis, such as high-mobility group protein B1, can activate fibroblasts and bone marrow-derived fibroblast-like cells. These cells, once activated, secrete large

408 amounts of ECM components like collagen, leading to tissue fibrosis(Kang et al., 2016; Wenzel et
409 al., 2017). For example, ferroptosis is considered a key pathological mechanism in liver and heart
410 fibrosis (Fang et al., 2020; Friedmann Angeli et al., 2014).
411 Moreover, ROS and lipid peroxides produced during ferroptosis not only directly cause cell
412 damage but also induce inflammatory responses that further exacerbate fibrosis. For instance,
413 ROS generated by ferroptosis can activate nuclear factor kappa B (NF-κB) and other
414 pro-inflammatory signaling pathways, promoting the release of pro-fibrotic factors (Dixon et al.,
415 2012; Stockwell et al., 2017). Synthesizing these studies, it is evident that ferroptosis exacerbates
416 tissue fibrosis through inducing inflammatory responses, activating fibroblasts, and increasing
417 oxidative stress. These mechanisms provide important theoretical foundations for understanding
418 the role of ferroptosis in fibrotic diseases and developing new therapeutic strategies.

419 Prussian blue staining revealed a significant increase in iron accumulation in the skeletal muscles
420 of high-fat diet-induced obese mice. Obesity is often accompanied by systemic metabolic
421 disorders, including altered iron metabolism. Studies have shown that obese individuals often
422 exhibit lower serum iron levels and elevated hepcidin levels (Ganz, 2012). This increase in
423 hepcidin inhibits iron absorption and release, leading to iron accumulation in the body (Ganz,
424 2012). Additionally, pro-inflammatory factors secreted in obesity, such as TNF-α and IL-6, not
425 only stimulate hepcidin synthesis but also directly affect iron metabolism, increasing iron
426 accumulation in cells and tissues (Hotamisligil, 2006; Weisberg et al., 2003). These findings are
427 consistent with what we observed in the skeletal muscles of high-fat diet-induced obese mice.
428 Ferroptosis is an iron-dependent form of cell death, and its extent can be reflected by the amount
429 of iron accumulation in cells, tissues, and organs. Iron accumulation is a critical trigger for
430 ferroptosis. Excess intracellular iron generates large amounts of ROS through the Fenton Reaction,
431 which induce lipid peroxidation and thereby trigger ferroptosis (Dixon et al., 2012; Stockwell et
432 al., 2017). These research findings strongly support that ferroptosis is accompanied by iron
433 accumulation.

434 IHC revealed a significant increase in the expression of 4-HNE and MDA in the skeletal muscles
435 of high-fat diet-induced obese mice. 4-HNE is a highly reactive aldehyde compound produced by
436 lipid peroxidation, primarily derived from the peroxidation of ω-6 polyunsaturated fatty acids
437 (Ayala et al., 2014). It can form adducts with proteins, DNA, and phospholipids, altering their
438 structure and function, thereby causing cellular damage (Murdolo et al., 2023). Studies have
439 shown that the levels of 4-HNE are significantly elevated in obese individuals, indicating the role
440 of lipid peroxidation in obesity (Guo et al., 2017; Murdolo et al., 2023). Similarly, MDA, another
441 product of lipid peroxidation, is commonly used to measure oxidative stress levels. High levels of
442 MDA indicate lipid damage to cell membranes and altered cellular function (Ahmed et al., 2016;
443 Savira et al., 2020). As with 4-HNE, elevated levels of MDA have been observed in obese
444 individuals (Ahmed et al., 2016; Savira et al., 2020).
445 Ferroptosis is accompanied by the accumulation of lipid peroxides and oxidative stress (Dixon et
446 al., 2012). This process is closely related to the expression of 4-HNE and MDA, as both
447 compounds are markers of lipid peroxidation (He et al., 2022; Park et al., 2021). During
448 iron-catalyzed lipid peroxidation, large amounts of ROS are produced, with 4-HNE and MDA
449 being key lipid peroxides. These compounds can react with phospholipids, proteins, and DNA in

cell membranes, leading to membrane damage, loss of protein function, and DNA damage, ultimately resulting in cell death (He et al., 2022; Weber & Lanci, 2021). Iron generates highly reactive hydroxyl radicals (•OH) through the Fenton Reaction, which further induce lipid peroxidation, increasing the production of 4-HNE and MDA, enhancing oxidative stress within cells, and promoting ferroptosis (Endale et al., 2023). Furthermore, 4-HNE is not only a product of lipid peroxidation but also an important signaling molecule that can regulate various cellular processes, including inflammatory responses, cell proliferation, and apoptosis (Park et al., 2021). In summary, 4-HNE and MDA play critical roles as markers of lipid peroxidation in the process of ferroptosis.

In summary, high-fat diet-induced obesity leads to inflammation cell infiltration, fibrosis, iron metabolism dysregulation, and increased lipid peroxides in skeletal muscle. These negative factors collectively contribute to the occurrence of ferroptosis in skeletal muscle.

4.3 Regulation of GPX4 in White Muscle by Obesity.

To better explore the regulatory mechanisms of ferroptosis in skeletal muscle induced by obesity, we used WB to examine the expression of ferroptosis signaling pathways in different types of muscle. GPX4 plays a key regulatory role in ferroptosis through amino acid metabolism by inhibiting the cell death process via the reduction of lipid peroxides accumulation (Stockwell et al., 2017). The deficiency or inactivation of GPX4 leads to an increase in lipid peroxides, thereby triggering ferroptosis (W. S. Yang et al., 2014).

Under normal dietary conditions, the expression of GPX4 is significantly higher in white muscle compared to red muscle. This may be due to the higher metabolic activity and oxidative stress levels in white muscle, which require more antioxidant protection to maintain cellular homeostasis (Brennan, 2008; Kitase et al., 2018). Furthermore, the fiber type of white muscle has higher oxidative metabolic demands and ROS generation, further promoting the increased expression of GPX4 to prevent damage caused by lipid peroxidation (Wesolowski et al., 2022).

However, under the high-fat diet-induced obesity, the expression of GPX4 in white muscle significantly decreases, while its expression in red muscle remains unaffected. This may be due to the higher sensitivity of white muscle to lipid peroxidation. A high-fat diet increases oxidative stress in white muscle, leading to GPX4 depletion, whereas red muscle, with its stronger antioxidant capacity, can maintain GPX4 levels (Katunga et al., 2015; Zhuang et al., 2021). Additionally, higher metabolic activity and lipid accumulation in white muscle may also contribute to the significant decrease in GPX4 expression (Shi et al., 2024).

4.4 Regulation of NCOA4 in Red Muscle by Obesity.

NCOA4 mediates ferritinophagy, the process of degrading ferritin to release stored iron, thereby increasing intracellular free iron content. This promotes iron-catalyzed Fenton Reactions, leading to lipid peroxidation and ferroptosis (Dowdle et al., 2014; Mancias et al., 2014). Studies have shown that the absence of NCOA4 significantly reduces the occurrence of ferroptosis, further demonstrating its crucial role in the ferroptosis process (Dowdle et al., 2014; Mancias et al., 2014).

Under normal conditions, the expression of NCOA4 is significantly higher in white muscle compared to red muscle. This may be due to the higher metabolic activity and iron demand in white muscle, necessitating higher levels of NCOA4 to regulate iron metabolism and storage, thus

meeting the energy needs during high-intensity, short-duration contractions (Muckenthaler et al., 2017; Palstra et al., 2013). Additionally, NCOA4 plays a vital role in maintaining iron homeostasis and promoting muscle function in metabolically active white muscle by releasing iron from ferritin through ferritinophagy (Gehrer et al., 2023).

However, a high-fat diet induced obesity impacts the expression of NCOA4 differently in red and white muscles, with an increase in red muscle and a significant decrease in white muscle. White muscle primarily relies on anaerobic metabolism and is more sensitive to lipid peroxidation and metabolic stress. The increased metabolic stress caused by a high-fat diet enhances the white muscle cells' need for oxidative stress defense, possibly downregulating NCOA4 expression to reduce ferritinophagy activities, thereby protecting the cells damage from further ferroptosis. This hypothesis requires further in-depth research.

4.5 Red and White Muscle Regulate 4-HNE Through NCOA4 and GPX4

Under normal conditions, the expression of 4-HNE in white muscle is lower than in red muscle. This may be due to the higher oxidative metabolism rate and mitochondrial content in red muscle, leading to increased generation of ROS, which trigger more lipid peroxidation reactions and produce more 4-HNE (Morris et al., 2008; Paglialunga et al., 2015). Additionally, the antioxidant defense mechanisms in red muscle are relatively weaker, resulting in lower clearance efficiency of lipid peroxidation products like 4-HNE, further increasing its accumulation in red muscle (Hart et al., 2018).

A high-fat diet-induced obesity leads to increased lipid accumulation and oxidative stress in both red and white muscles, significantly enhancing the production of 4-HNE (Hart et al., 2018; Shi et al., 2024). This diet also weakens antioxidant defense mechanisms, such as reducing the activity of glutathione and superoxide dismutase, further exacerbating lipid peroxidation (Hart et al., 2018). It is of paramount importance to note that the skeletal muscle type specific expression of GPX4 and NCOA4 as upstream and regulatory signals of 4-HNE was significantly modulated by high-fat-induced obesity. Consequently, we propose that the upregulation of 4-HNE in red and white muscle due to high-fat induced obesity is caused by significant alterations in the expression of NCOA4 and GPX4, separately.

4.6 Obesity and Muscle Type do not Alter MDA Expression

After a high-fat diet, the expression of 4-HNE significantly increased in both red and white muscles, whereas the expression of MDA did not show significant changes. This discrepancy may be due to the differences in the generation and metabolism processes of 4-HNE and MDA. The production of 4-HNE is highly influenced by ROS. A high-fat diet increases lipid peroxidation reactions and ROS production, thereby significantly elevating 4-HNE levels (Morris et al., 2008; Ramana et al., 2014). Additionally, 4-HNE is highly reactive and can form stable adducts with various biomolecules such as proteins, DNA, and phospholipids, leading to its accumulation in tissues (Ayala et al., 2014; Morris et al., 2008). However, the production of MDA is relatively stable, and its metabolic pathways are more diverse and efficient. For example, MDA can be metabolized through various pathways, such as being converted into water-soluble products by glutathione-S-transferase for excretion or being transformed into less reactive compounds (Esterbauer et al., 1991). These metabolic pathways make it less likely for MDA levels to show significant changes under high-fat diet conditions (Del Rio et al., 2005).

Furthermore, some studies suggest that MDA is more likely to be rapidly produced and cleared under acute oxidative stress conditions rather than accumulating under chronic conditions (Del Rio et al., 2005). Previous studies have found that, after a high-fat diet, the expression of 4-HNE significantly increased in some cells, tissues, and organs, while the expression of MDA did not show significant changes (Bastin et al., 1990; Chung et al., 2018; Maciejczyk et al., 2018; Tanaka et al., 2008). These studies indicate that due to the more diverse and efficient metabolic and clearance mechanisms of MDA, its levels may not significantly change in certain tissues and organs.

Additionally, experimental techniques can affect the expression of MDA. When using IHC and WB to detect MDA, IHC showed a significant increase in MDA after a high-fat diet, whereas WB did not show the same results. This discrepancy may arise from differences in the sensitivity and specificity of the detection methods (Del Rio et al., 2005). IHC can detect local accumulation of MDA in specific cell types or tissue regions, while WB measures overall protein levels, which may dilute signals of local high expression. Furthermore, differences in sample processing and extraction methods may lead to dilution or degradation of locally high concentrations of MDA in WB, affecting the detection results. These factors collectively explain why IHC can show a significant increase in MDA after a high-fat diet, while WB does not detect the same changes.

4.8 Regulation of Ferroptosis by DR and DR+Ex

We found that intervention with a DR did not improve the obesity-induced changes in body composition and skeletal muscle dysfunction. The main reasons may include the following points. Firstly, obesity is often accompanied by chronic low-grade inflammation, which can lead to skeletal muscle dysfunction and adverse changes in body composition (Pedersen & Febbraio, 2008). A 20% DR may not be sufficient to significantly reduce inflammation levels. Secondly, a high-fat diet leads to insulin resistance (Samuel & Shulman, 2012). Insulin resistance not only affects glucose metabolism but also reduces muscle protein synthesis, thereby impacting skeletal muscle function (Wilkinson et al., 2013). Thus, a 20% DR may not be enough to significantly improve insulin sensitivity. Additionally, the metabolic disorders caused by obesity usually require a longer duration and a greater degree of dietary intervention to reverse. A 20% high-fat dietary restriction in terms of time and extent may not be sufficient to achieve the desired effects (Astrup et al., 2008). Intervention with a 20% DR+Ex partially improved body composition but not skeletal muscle function. This is because exercise can increase energy expenditure, promote fat oxidation, and improve metabolic function (Hill & Wyatt, 2005). However, improving skeletal muscle function requires a longer duration and specific types of stimuli, such as resistance training, rather than just aerobic exercise (Kelley, 1998).

H&E staining showed that an DR and DR+Ex reduced inflammatory cell infiltration in skeletal muscle. This is due to the anti-inflammatory effects of DR and Ex. However, Masson's trichrome staining showed that these interventions did not reduce fibrosis in the skeletal muscles of obese mice, likely because the pathological process of fibrosis is complex and difficult to significantly affect with short-term interventions (Gillies & Lieber, 2011). Additionally, dietary adjustments may not have been comprehensive enough, and the type and intensity of exercise may have been insufficient to effectively inhibit fibrosis formation (Bonnard et al., 2008). Similarly, these interventions did not reduce iron accumulation in the skeletal muscles of obese mice. This could

be due to insufficient dietary adjustments and exercise intensity and type, which may not have significantly impacted iron metabolism (McClung & Karl, 2009). Moreover, iron accumulation is a long-term process, and short-term interventions are unlikely to change existing iron deposits (Domellöf et al., 2018). Finally, the diet may have lacked key nutrients such as vitamin C, which can affect iron absorption and regulation (Zimmermann & Hurrell, 2007).

After DR and DR+Ex, the expression of 4-HNE and MDA in the skeletal muscles of obese mice did not decrease. This may be attributed to the complexity of metabolic adaptation, oxidative stress, and antioxidant mechanisms, as well as the diverse effects of different interventions on skeletal muscle. Firstly, diet and exercise may lead to complex metabolic adaptations in skeletal muscle. Studies have shown that although a high-fat diet induces obesity and insulin resistance, it does not significantly alter the transcriptome expression in skeletal muscle, indicating that gene expression changes under such interventions are minimal and difficult to detect (de Wilde et al., 2009). Secondly, in the state of obesity, the levels of oxidative stress may already be very high, and DR or DR+Ex alone may not be sufficient to significantly reduce the production of 4-HNE and MDA. Research has shown that while DR and Ex improve metabolic indicators and skeletal muscle function, they do not significantly alter the levels of specific oxidative stress markers (J. H. Lee et al., 2021). Lastly, the effects of exercise and diet on skeletal muscle are diverse. Some studies suggest that DR and Ex can improve obesity and insulin resistance, but the specific effects on mitochondrial function and oxidative stress in skeletal muscle are complex, requiring further research to clarify the comprehensive effects of these interventions (Pattanakuhar et al., 2019). These factors may collectively contribute to the stability of 4-HNE and MDA levels in skeletal muscle.

4.9 DR+Ex Regulated GPX4 Expression in Red Muscle

Although no significant regulatory effects of DR and DR+Ex on ferroptosis signals (4-HNE and MDA) in the wholly skeletal muscles of obese mice were found, some regulatory trends did emerge. Therefore, we used WB analysis to examine the regulatory mechanisms of DR and DR+Ex on ferroptosis signals in different muscle types. The results showed that after DR+Ex, the expression of GPX4 in red muscle significantly increased in obese mice, whereas it did not in white muscle. This may be related to the oxidative stress, metabolic demands, and specific gene regulatory mechanisms of different skeletal muscle types.

Firstly, red muscle primarily relies on aerobic metabolism and is rich in mitochondria, adapting to prolonged low-intensity exercise. Therefore, its antioxidant mechanisms are more active to cope with higher levels of oxidative stress. Studies have shown that antioxidant mechanisms in red muscle are more prominent, potentially leading to the easier expression of GPX4 in response to oxidative stress in this environment (Rinnankoski-Tuikka et al., 2012). Secondly, DR and Ex lead to increased metabolic activity in skeletal muscle, requiring more antioxidant protection to prevent lipid peroxidation damage (Civitarese et al., 2007; Galassetti et al., 2006). As a key antioxidant enzyme, GPX4 is upregulated in this context, while white muscle, which primarily relies on glycolysis for energy, has lower oxidative stress, and its GPX4 expression maybe does not significantly increase. Lastly, DR and Ex can regulate gene expression through specific signaling pathways such as AMPK and PGC-1α. These pathways are more active in red muscle (Gouspillou et al., 2014; Jørgensen et al., 2007; Pengam et al., 2020) and are related to the expression of

antioxidant enzymes.

In summary, the increased expression of GPX4 in red muscle may be due to its high sensitivity to oxidative stress, higher metabolic demands, and specific gene regulation induced by exercise. In contrast, white muscle, with its different metabolic characteristics and lower oxidative stress levels, did not show the same changes in GPX4 expression.

4.10 DR and DR+Ex Regulated AMPK Expression in White Muscle

We found that after DR+Ex in obese mice, the expression of AMPK decreased in white muscle but not in red muscle. This may be related to the metabolic differences between muscle fiber types, exercise-induced specific regulation, and the different impacts of diet and exercise on metabolic regulation.

Red muscle primarily relies on aerobic metabolism, is rich in mitochondria, and is adapted to prolonged low-intensity exercise, maintaining high AMPK activity to meet its metabolic demands and antioxidant capacity. Under conditions of exercise and dietary restriction, AMPK expression remains stable in red muscle. In contrast, white muscle primarily relies on glycolysis for energy, has lower oxidative stress, and therefore requires less AMPK, leading to a possible decrease in its expression (Jørgensen et al., 2007).

Additionally, exercise regulates gene expression through specific signaling pathways such as AMPK and PGC-1α, which are more active and abundant in red muscle, thereby maintaining its expression levels. However, in white muscle, lower AMPK activity leads to a reduction in its expression (Sriwijitkamol et al., 2006). Lastly, the effects of a high-fat diet and exercise on metabolic regulation differ between muscle fiber types. In red muscle, dietary restriction and exercise can maintain high metabolic activity and antioxidant capacity, whereas in white muscle, these regulatory effects are weaker, leading to a decrease in AMPK expression (J.-H. Lee et al., 2021).

4.11 DR and DR+Ex Led to a Decrease in 4-HNE Expression in Red Muscle

After DR and DR+Ex in obese mice, the expression of 4-HNE decreased in red muscle but not in white muscle. This difference is related to the metabolic differences between skeletal muscle types, specific gene regulation, and the specific effects of diet and exercise on red muscle.

Red muscle primarily relies on aerobic metabolism, is rich in mitochondria, and is adapted to prolonged low-intensity exercise. Consequently, its metabolic activity and oxidative stress are higher, necessitating stronger antioxidant protection mechanisms. Studies have shown that red muscle significantly increases antioxidant enzyme activity under DR and Ex, reducing the production of oxidative stress markers such as 4-HNE (Jørgensen et al., 2007). Moreover, exercise regulates gene expression through specific signaling pathways which are more active in red muscle. This promotes the expression and activity of antioxidant enzymes, further reducing levels of oxidative stress markers (Sriwijitkamol et al., 2006).

We found that as an upstream signal and regulatory molecule of 4-HEN, the expression of GPX4 in red muscle significantly increased after intervention. Therefore, we propose that DR and DR+Ex can regulate ferroptosis by altering the expression of GPX4 in red muscle, which in turn modulates the downstream expression of 4-HEN. However, AMPK, also an upstream regulatory molecule of 4-HEN, showed inconsistent expression changes with 4-HNE in white muscle. After a high-fat diet, the regulatory effect of AMPK on 4-HNE in white muscle was impaired, likely due

to metabolic disturbances caused by obesity. This warrants further investigation in future studies.

5. Conclusion

Obesity induced by a high-fat diet leads to ferroptosis in the skeletal muscle of mice. The mechanism is muscle type-specific, with NCOA4 expression upregulated in red muscle and GPX4 expression upregulated in white muscle, ultimately triggering ferroptosis. Additionally, DR and DR+Ex can partially mitigate ferroptosis in the skeletal muscle of obese mice induced by a high-fat diet. This mechanism is achieved by regulating the expression of GPX4 in red muscle. Overall, we have identified muscle type-specific regulatory mechanisms of ferroptosis, providing molecular biology-related scientific data for the prevention and treatment of related diseases in the future.

6. limitation

The study focuses on the gastrocnemius muscle, which may not fully represent the effects of dietary restriction and exercise on other muscle groups, as different muscles may respond differently to these interventions. Additionally, the duration of dietary restriction and exercise intervention was limited to eight weeks. Longer-term studies are necessary to understand the chronic effects and sustainability of these interventions on ferroptosis and overall muscle health. Furthermore, incorporating advanced experimental tools, such as single-cell sequencing, could provide a more detailed and microscopic analysis of the results.

7. WB representative picture

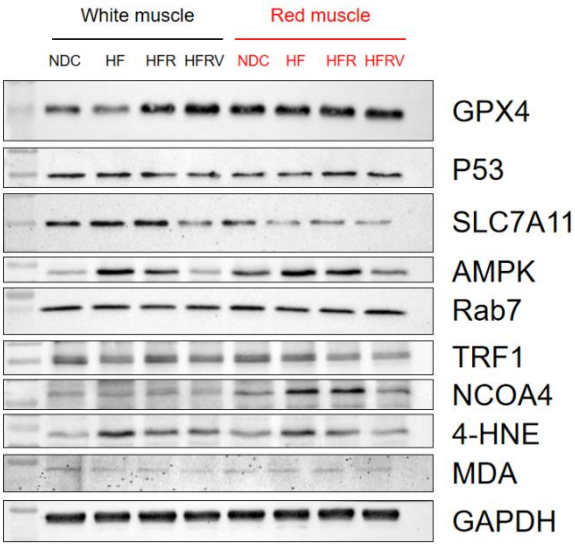

8. Ethical approval and consent to participate

All the procedures followed in this experiment were approved by the Institutional Animal Care and Use Committee (IACUC) of Hanyang University (HYU 2021-0066A).

9. Consent for publication

Not applicable.

10. Availability of data and materials

The data used to support the findings of this study are presented here. Any further data requirements are available from the corresponding author upon request.

11. Competing interests

No conflicts of interest, financial or otherwise, have been declared by the author(s).

12. Funding

This research was supported by the National Research Foundation of Korea (NRF-2020R1F1A1061726).

13. Author's contributions

F.J.J. and J.H.K. conceived and designed the study. F.J.J., Y.J.P. and H.s.L. performed the experiments. F.J.J. and H.s.L. analyzed the data and prepared the figures. F.J.J. and J.H.K. interpreted the results, drafted, edited, and revised the manuscript. J.H.K. acquired funding. All authors approved the final version of the manuscript.

14. Acknowledgments

We thank Jian Guo (Hanyang University, Korea) for his generous help in dissecting the mice.

We are grateful to Prof. Dr. Gwang-woong Go (Hanyang University, Korea) for generously providing the DEXA machine for body composition analysis of the mice.

We thank the support of Skill Learning from Kaixin Doctor and MASCU (Medical Association with Science, Creativity, and Unity), Inc, Shenzhen, China (mascu_forever@163.com).

15. Reference

Ahmed, S., Maher, F., & Naji, N. (2016). Effect of leptin and oxidative stress in the blood of obese individuals. *Biochem Anal Biochem*, *5*(288), 2161-1009.

Alghannam, A. F., Jedrzejewski, D., Tweddle, M., Gribble, H., Bilzon, J. L., & Betts, J. A. (2016). Reliability of Time to Exhaustion Treadmill Running as a Measure of Human Endurance Capacity. *Int J Sports Med*, *37*(3), 219-223. https://doi.org/10.1055/s-0035-1555928

Armani, A., Cinti, F., Marzolla, V., Morgan, J., Cranston, G. A., Antelmi, A., Carpinelli, G., Canese, R., Pagotto, U., & Quarta, C. (2014). Mineralocorticoid receptor antagonism induces browning of white adipose tissue through impairment of autophagy and prevents adipocyte dysfunction in high-fat-diet-fed mice. *The FASEB Journal*, *28*(8), 3745-3757.

Astrup, A., Dyerberg, J., Selleck, M., & Stender, S. (2008). Nutrition transition and its relationship to the development of obesity and related chronic diseases. *Obes Rev*, *9 Suppl 1*, 48-52. https://doi.org/10.1111/j.1467-789X.2007.00438.x

Ayala, A., Muñoz, M. F., & Argüelles, S. (2014). Lipid peroxidation: production, metabolism, and signaling mechanisms of malondialdehyde and 4-hydroxy-2-nonenal. *Oxidative Medicine and Cellular Longevity*, *2014*.

Bastin, J., Djouadi, F., Geloso, J. P., & Merlet-Benichou, C. (1990). Postnatal development of oxidative enzymes in various rat nephron segments: effect of weaning on different diets. *Am J Physiol*, *259*(6 Pt 2), F895-901. https://doi.org/10.1152/ajprenal.1990.259.6.F895

722 Bevilacqua, L., Ramsey, J. J., Hagopian, K., Weindruch, R., & Harper, M.-E. (2005). Long-term caloric
723 restriction increases UCP3 content but decreases proton leak and reactive oxygen species
724 production in rat skeletal muscle mitochondria. *American Journal of*
725 *Physiology-Endocrinology and Metabolism*, *289*(3), E429-E438.
726 Blüher, M. (2019). Obesity: global epidemiology and pathogenesis. *Nature Reviews Endocrinology*,
727 *15*(5), 288-298.
728 Bonnard, C., Durand, A., Peyrol, S., Chanseaume, E., Chauvin, M. A., Morio, B., Vidal, H., & Rieusset, J.
729 (2008). Mitochondrial dysfunction results from oxidative stress in the skeletal muscle of
730 diet-induced insulin-resistant mice. *J Clin Invest*, *118*(2), 789-800.
731 https://doi.org/10.1172/jci32601
732 Brennan, K. M. (2008). *Antioxidant gene expression and mitochondrial function during [beta]-oxidation*
733 *in beef cattle* Washington State University].
734 Buettner, R., Schölmerich, J., & Bollheimer, L. C. (2007). High-fat diets: modeling the metabolic
735 disorders of human obesity in rodents. *Obesity*, *15*(4), 798-808.
736 Chen, D., Wang, Y., & Chin, E. R. (2015). Activation of the endoplasmic reticulum stress response in
737 skeletal muscle of G93A*SOD1 amyotrophic lateral sclerosis mice. *Front Cell Neurosci*, *9*, 170.
738 https://doi.org/10.3389/fncel.2015.00170
739 Chen, J., Zhu, T., Yu, D., Yan, B., Zhang, Y., Jin, J., Yang, Z., Zhang, B., Hao, X., & Chen, Z. (2023).
740 Moderate intensity of treadmill exercise rescues TBI-induced ferroptosis, neurodegeneration,
741 and cognitive impairments via suppressing STING pathway. *Molecular Neurobiology*, *60*(9),
742 4872-4896.
743 Chen, W., Wilson, J. L., Khaksari, M., Cowley, M. A., & Enriori, P. J. (2012). Abdominal fat analyzed by
744 DEXA scan reflects visceral body fat and improves the phenotype description and the
745 assessment of metabolic risk in mice. *Am J Physiol Endocrinol Metab*, *303*(5), E635-643.
746 https://doi.org/10.1152/ajpendo.00078.2012
747 Chen, X., Comish, P. B., Tang, D., & Kang, R. (2021). Characteristics and Biomarkers of Ferroptosis.
748 *Front Cell Dev Biol*, *9*, 637162. https://doi.org/10.3389/fcell.2021.637162
749 Chooi, Y. C., Ding, C., & Magkos, F. (2019). The epidemiology of obesity. *Metabolism*, *92*, 6-10.
750 https://doi.org/10.1016/j.metabol.2018.09.005
751 Chung, A., Gurtu, S., Chakravarthi, S., Moorthy, M., & Palanisamy, U. D. (2018). Geraniin Protects
752 High-Fat Diet-Induced Oxidative Stress in Sprague Dawley Rats. *Front Nutr*, *5*, 17.
753 https://doi.org/10.3389/fnut.2018.00017
754 Civitarese, A. E., Carling, S., Heilbronn, L. K., Hulver, M. H., Ukropcova, B., Deutsch, W. A., Smith, S. R.,
755 & Ravussin, E. (2007). Calorie restriction increases muscle mitochondrial biogenesis in
756 healthy humans. *PLoS medicine*, *4*(3), e76.
757 Dächert, J., Ehrenfeld, V., Habermann, K., Dolgikh, N., & Fulda, S. (2020). Targeting ferroptosis in
758 rhabdomyosarcoma cells. *Int J Cancer*, *146*(2), 510-520. https://doi.org/10.1002/ijc.32496
759 de Wilde, J., Smit, E., Mohren, R., Boekschoten, M. V., de Groot, P., van den Berg, S. A., Bijland, S.,
760 Voshol, P. J., van Dijk, K. W., de Wit, N. W., Bunschoten, A., Schaart, G., Hulshof, M. F., &
761 Mariman, E. C. (2009). An 8-week high-fat diet induces obesity and insulin resistance with
762 small changes in the muscle transcriptome of C57BL/6J mice. *J Nutrigenet Nutrigenomics*,
763 *2*(6), 280-291. https://doi.org/10.1159/000308466

764 Del Rio, D., Stewart, A. J., & Pellegrini, N. (2005). A review of recent studies on malondialdehyde as
765 toxic molecule and biological marker of oxidative stress. *Nutr Metab Cardiovasc Dis*, *15*(4),
766 316-328. https://doi.org/10.1016/j.numecd.2005.05.003
767 Ding, H., Chen, S., Pan, X., Dai, X., Pan, G., Li, Z., Mai, X., Tian, Y., Zhang, S., Liu, B., Cao, G., Yao, Z., Yao,
768 X., Gao, L., Yang, L., Chen, X., Sun, J., Chen, H., Han, M., . . . Xie, L. (2021). Transferrin receptor
769 1 ablation in satellite cells impedes skeletal muscle regeneration through activation of
770 ferroptosis. *J Cachexia Sarcopenia Muscle*, *12*(3), 746-768.
771 https://doi.org/10.1002/jcsm.12700
772 Dixon, S. J., Lemberg, K. M., Lamprecht, M. R., Skouta, R., Zaitsev, E. M., Gleason, C. E., Patel, D. N.,
773 Bauer, A. J., Cantley, A. M., & Yang, W. S. (2012). Ferroptosis: an iron-dependent form of
774 nonapoptotic cell death. *cell*, *149*(5), 1060-1072.
775 Domellöf, M., Szitanyi, P., Simchowitz, V., Franz, A., & Mimouni, F. (2018).
776 ESPGHAN/ESPEN/ESPR/CSPEN guidelines on pediatric parenteral nutrition: Iron and trace
777 minerals. *Clin Nutr*, *37*(6 Pt B), 2354-2359. https://doi.org/10.1016/j.clnu.2018.06.949
778 Dowdle, W. E., Nyfeler, B., Nagel, J., Elling, R. A., Liu, S., Triantafellow, E., Menon, S., Wang, Z., Honda,
779 A., Pardee, G., Cantwell, J., Luu, C., Cornella-Taracido, I., Harrington, E., Fekkes, P., Lei, H.,
780 Fang, Q., Digan, M. E., Burdick, D., . . . Murphy, L. O. (2014). Selective VPS34 inhibitor blocks
781 autophagy and uncovers a role for NCOA4 in ferritin degradation and iron homeostasis in vivo.
782 *Nature cell biology*, *16*(11), 1069-1079. https://doi.org/10.1038/ncb3053
783 Endale, H. T., Tesfaye, W., & Mengstie, T. A. (2023). ROS induced lipid peroxidation and their role in
784 ferroptosis. *Frontiers in cell and Developmental Biology*, *11*.
785 Esterbauer, H., Schaur, R. J., & Zollner, H. (1991). Chemistry and biochemistry of 4-hydroxynonenal,
786 malonaldehyde and related aldehydes. *Free Radic Biol Med*, *11*(1), 81-128.
787 https://doi.org/10.1016/0891-5849(91)90192-6
788 Fang, X., Cai, Z., Wang, H., Han, D., Cheng, Q., Zhang, P., Gao, F., Yu, Y., Song, Z., & Wu, Q. (2020). Loss
789 of cardiac ferritin H facilitates cardiomyopathy via Slc7a11-mediated ferroptosis. *Circulation*
790 *research*, *127*(4), 486-501.
791 Friedmann Angeli, J. P., Schneider, M., Proneth, B., Tyurina, Y. Y., Tyurin, V. A., Hammond, V. J., Herbach,
792 N., Aichler, M., Walch, A., & Eggenhofer, E. (2014). Inactivation of the ferroptosis regulator
793 Gpx4 triggers acute renal failure in mice. *Nature cell biology*, *16*(12), 1180-1191.
794 Galassetti, P. R., Nemet, D., Pescatello, A., Rose-Gottron, C., Larson, J., & Cooper, D. M. (2006). Exercise,
795 caloric restriction, and systemic oxidative stress. *Journal of investigative medicine*, *54*(2),
796 67-75.
797 Ganz, T. (2012). Macrophages and systemic iron homeostasis. *Journal of innate immunity*, *4*(5-6),
798 446-453.
799 Gehrer, C. M., Mitterstiller, A. M., Grubwieser, P., Meyron-Holtz, E. G., Weiss, G., & Nairz, M. (2023).
800 Advances in Ferritin Physiology and Possible Implications in Bacterial Infection. *Int J Mol Sci*,
801 *24*(5). https://doi.org/10.3390/ijms24054659
802 Gillies, A. R., & Lieber, R. L. (2011). Structure and function of the skeletal muscle extracellular matrix.
803 *Muscle Nerve*, *44*(3), 318-331. https://doi.org/10.1002/mus.22094
804 Gouspillou, G., Sgarioto, N., Norris, B., Barbat-Artigas, S., Aubertin-Leheudre, M., Morais, J. A., Burelle,
805 Y., Taivassalo, T., & Hepple, R. T. (2014). The relationship between muscle fiber type-specific
806 PGC-1α content and mitochondrial content varies between rodent models and humans. *PloS*
807 *one*, *9*(8), e103044. https://doi.org/10.1371/journal.pone.0103044

808 Graber, T. G., Ferguson-Stegall, L., Kim, J. H., & Thompson, L. V. (2013). C57BL/6 neuromuscular
809 healthspan scoring system. *J Gerontol A Biol Sci Med Sci*, *68*(11), 1326-1336.
810 https://doi.org/10.1093/gerona/glt032
811 Graham, L. C., Grabowska, W. A., Chun, Y., Risacher, S. L., Philip, V. M., Saykin, A. J., Rizzo, S. J. S.,
812 Howell, G. R., & Initiative, A. s. D. N. (2019). Exercise prevents obesity-induced cognitive
813 decline and white matter damage in mice. *Neurobiology of aging*, *80*, 154-172.
814 Guerrero-Hue, M., García-Caballero, C., Palomino-Antolín, A., Rubio-Navarro, A., Vázquez-Carballo, C.,
815 Herencia, C., Martín-Sanchez, D., Farré-Alins, V., Egea, J., Cannata, P., Praga, M., Ortiz, A.,
816 Egido, J., Sanz, A. B., & Moreno, J. A. (2019). Curcumin reduces renal damage associated with
817 rhabdomyolysis by decreasing ferroptosis-mediated cell death. *Faseb j*, *33*(8), 8961-8975.
818 https://doi.org/10.1096/fj.201900077R
819 Guo, L., Zhang, X.-M., Zhang, Y.-B., Huang, X., & Chi, M.-H. (2017). Association of 4-hydroxynonenal
820 with classical adipokines and insulin resistance in a Chinese non-diabetic obese population.
821 *Nutricion hospitalaria*, *34*(2), 363-368.
822 Han, C., Lee, S., Lim, S., Kong, H., Kim, S., Lee, S., & Chang, J. (2006). Studies on production of high fat
823 diet induced obesity C57BL/6NCrjBgi mice. *Laboratory Animal Research*, *22*(3), 221-226.
824 Han, C., Liu, Y., Dai, R., Ismail, N., Su, W., & Li, B. (2020). Ferroptosis and its potential role in human
825 diseases. *Frontiers in pharmacology*, *11*, 239.
826 Hariri, N., & Thibault, L. (2010). High-fat diet-induced obesity in animal models. *Nutrition research*
827 *reviews*, *23*(2), 270-299.
828 Hart, C. R., Layec, G., Trinity, J. D., Kwon, O. S., Zhao, J., Reese, V. R., Gifford, J. R., & Richardson, R. S.
829 (2018). Increased skeletal muscle mitochondrial free radical production in peripheral arterial
830 disease despite preserved mitochondrial respiratory capacity. *Exp Physiol*, *103*(6), 838-850.
831 https://doi.org/10.1113/ep086905
832 He, F., Huang, X., Wei, G., Lin, X., Zhang, W., Zhuang, W., He, W., Zhan, T., Hu, H., & Yang, H. (2022).
833 Regulation of ACSL4-catalyzed lipid peroxidation process resists cisplatin ototoxicity.
834 *Oxidative Medicine and Cellular Longevity*, *2022*.
835 Hill, J. O., & Wyatt, H. R. (2005). Role of physical activity in preventing and treating obesity. *J Appl*
836 *Physiol (1985)*, *99*(2), 765-770. https://doi.org/10.1152/japplphysiol.00137.2005
837 Hotamisligil, G. S. (2006). Inflammation and metabolic disorders. *Nature*, *444*(7121), 860-867.
838 Huang, Y., Wu, B., Shen, D., Chen, J., Yu, Z., & Chen, C. (2021). Ferroptosis in a sarcopenia model of
839 senescence accelerated mouse prone 8 (SAMP8). *Int J Biol Sci*, *17*(1), 151-162.
840 https://doi.org/10.7150/ijbs.53126
841 Jørgensen, S. B., Treebak, J. T., Viollet, B., Schjerling, P., Vaulont, S., Wojtaszewski, J. F., & Richter, E. A.
842 (2007). Role of AMPKα2 in basal, training-, and AICAR-induced GLUT4, hexokinase II, and
843 mitochondrial protein expression in mouse muscle. *American Journal of*
844 *Physiology-Endocrinology and Metabolism*, *292*(1), E331-E339.
845 Justice, J. N., Cesari, M., Seals, D. R., Shively, C. A., & Carter, C. S. (2016). Comparative Approaches to
846 Understanding the Relation Between Aging and Physical Function. *J Gerontol A Biol Sci Med*
847 *Sci*, *71*(10), 1243-1253. https://doi.org/10.1093/gerona/glv035
848 Kang, R., Zeng, L., Xie, Y., Yan, Z., Zhou, B., Cao, L., Klionsky, D. J., Tracey, K. J., Li, J., & Wang, H. (2016).
849 A novel PINK1-and PARK2-dependent protective neuroimmune pathway in lethal sepsis.
850 *Autophagy*, *12*(12), 2374-2385.

851 Katunga, L. A., Gudimella, P., Efird, J. T., Abernathy, S., Mattox, T. A., Beatty, C., Darden, T. M., Thayne, K.
852 A., Alwair, H., Kypson, A. P., Virag, J. A., & Anderson, E. J. (2015). Obesity in a model of gpx4
853 haploinsufficiency uncovers a causal role for lipid-derived aldehydes in human metabolic
854 disease and cardiomyopathy. *Mol Metab*, *4*(6), 493-506.
855 https://doi.org/10.1016/j.molmet.2015.04.001
856 Kelley, G. A. (1998). Aerobic exercise and bone density at the hip in postmenopausal women: a
857 meta-analysis. *Prev Med*, *27*(6), 798-807. https://doi.org/10.1006/pmed.1998.0360
858 Khachatoorian, Y., & Samara, A. (2018). Differential effects of dietary restriction combined with
859 exercise vs dietary restriction alone on visceral and subcutaneous adipose tissues: A
860 systematic review. *Obesity Medicine*, *9*, 7-17.
861 Kim, J. D., McCarter, R. J., & Yu, B. P. (1996). Influence of age, exercise, and dietary restriction on
862 oxidative stress in rats. *Aging (Milano)*, *8*(2), 123-129. https://doi.org/10.1007/bf03339566
863 Kitase, Y., Vallejo, J. A., Gutheil, W., Vemula, H., Jähn, K., Yi, J., Zhou, J., Brotto, M., & Bonewald, L. F.
864 (2018). β-aminoisobutyric Acid, l-BAIBA, Is a Muscle-Derived Osteocyte Survival Factor. *Cell*
865 *Rep*, *22*(6), 1531-1544. https://doi.org/10.1016/j.celrep.2018.01.041
866 Koza, R. A., Nikonova, L., Hogan, J., Rim, J. S., Mendoza, T., Faulk, C., Skaf, J., & Kozak, L. P. (2006).
867 Changes in gene expression foreshadow diet-induced obesity in genetically identical mice.
868 *PLoS Genet*, *2*(5), e81. https://doi.org/10.1371/journal.pgen.0020081
869 Kvedaras, M., Minderis, P., Krusnauskas, R., & Ratkevicius, A. (2020). Effects of ten-week 30% caloric
870 restriction on metabolic health and skeletal muscles of adult and old C57BL/6J mice.
871 *Mechanisms of Ageing and Development*, *190*, 111320.
872 Lee, J.-H., Zhang, D., Kwak, S.-E., Shin, H.-E., & Song, W. (2021). Effects of exercise and a high-fat,
873 high-sucrose restriction diet on metabolic indicators, Nr4a3, and mitochondria-associated
874 protein expression in the gastrocnemius muscles of mice with diet-induced obesity. *Journal of*
875 *Obesity & Metabolic Syndrome*, *30*(1), 44.
876 Lee, J. H., Zhang, D., Kwak, S. E., Shin, H. E., & Song, W. (2021). Effects of Exercise and a High-Fat,
877 High-Sucrose Restriction Diet on Metabolic Indicators, Nr4a3, and Mitochondria-Associated
878 Protein Expression in the Gastrocnemius Muscles of Mice with Diet-Induced Obesity. *J Obes*
879 *Metab Syndr*, *30*(1), 44-54. https://doi.org/10.7570/jomes20043
880 Leem, Y. H., Park, J. S., Park, J. E., Kim, D. Y., & Kim, H. S. (2022). Neurogenic effects of rotarod walking
881 exercise in subventricular zone, subgranular zone, and substantia nigra in MPTP-induced
882 Parkinson's disease mice. *Sci Rep*, *12*(1), 10544. https://doi.org/10.1038/s41598-022-14823-5
883 Li, C., Feng, F., Xiong, X., Li, R., & Chen, N. (2017). Exercise coupled with dietary restriction reduces
884 oxidative stress in male adolescents with obesity. *Journal of sports sciences*, *35*(7), 663-668.
885 Li, J., Cao, F., Yin, H.-l., Huang, Z.-j., Lin, Z.-t., Mao, N., Sun, B., & Wang, G. (2020). Ferroptosis: past,
886 present and future. *Cell Death & Disease*, *11*(2), 88.
887 Lin, P.-Y., Romsos, D. R., & Leveille, G. A. (1977). Food intake, body weight gain, and body composition
888 of the young obese (ob/ob) mouse. *The Journal of Nutrition*, *107*(9), 1715-1723.
889 Liu, C. K., Leng, X., Hsu, F. C., Kritchevsky, S. B., Ding, J., Earnest, C. P., Ferrucci, L., Goodpaster, B. H.,
890 Guralnik, J. M., Lenchik, L., Pahor, M., & Fielding, R. A. (2014). The impact of sarcopenia on a
891 physical activity intervention: the Lifestyle Interventions and Independence for Elders Pilot
892 Study (LIFE-P). *J Nutr Health Aging*, *18*(1), 59-64. https://doi.org/10.1007/s12603-013-0369-0

Liu, T., Cui, Y., Dong, S., Kong, X., Xu, X., Wang, Y., Wan, Q., & Wang, Q. (2022). Treadmill training reduces cerebral ischemia-reperfusion injury by inhibiting ferroptosis through activation of SLC7A11/GPX4. *Oxidative Medicine and Cellular Longevity*, *2022*.

Luo, Y., Chen, H., Liu, H., Jia, W., Yan, J., Ding, W., Zhang, Y., Xiao, Z., & Zhu, Z. (2020). Protective effects of ferroptosis inhibition on high fat diet-induced liver and renal injury in mice. *International Journal of Clinical and Experimental Pathology*, *13*(8), 2041.

Ma, X., Pham, V. T., Mori, H., MacDougald, O. A., Shah, Y. M., & Bodary, P. F. (2017). Iron elevation and adipose tissue remodeling in the epididymal depot of a mouse model of polygenic obesity. *PloS one*, *12*(6), e0179889.

Maciejczyk, M., Żebrowska, E., Zalewska, A., & Chabowski, A. (2018). Redox Balance, Antioxidant Defense, and Oxidative Damage in the Hypothalamus and Cerebral Cortex of Rats with High Fat Diet-Induced Insulin Resistance. *Oxid Med Cell Longev*, *2018*, 6940515. https://doi.org/10.1155/2018/6940515

Magaki, S., Hojat, S. A., Wei, B., So, A., & Yong, W. H. (2019). An Introduction to the Performance of Immunohistochemistry. *Methods Mol Biol*, *1897*, 289-298. https://doi.org/10.1007/978-1-4939-8935-5_25

Mancias, J. D., Wang, X., Gygi, S. P., Harper, J. W., & Kimmelman, A. C. (2014). Quantitative proteomics identifies NCOA4 as the cargo receptor mediating ferritinophagy. *Nature*, *509*(7498), 105-109.

Mandarim-de-Lacerda, C. A., Del Sol, M., Vazquez, B., & Aguila, M. B. (2021). Mice as an animal model for the study of adipose tissue and obesity. *Int J Morphol*, *39*(6), 1521-1528.

Manzanares, G., Brito-da-Silva, G., & Gandra, P. G. (2018). Voluntary wheel running: patterns and physiological effects in mice. *Braz J Med Biol Res*, *52*(1), e7830. https://doi.org/10.1590/1414-431x20187830

Mattson, M. P., Longo, V. D., & Harvie, M. (2017). Impact of intermittent fasting on health and disease processes. *Ageing research reviews*, *39*, 46-58.

McClung, J. P., & Karl, J. P. (2009). Iron deficiency and obesity: the contribution of inflammation and diminished iron absorption. *Nutr Rev*, *67*(2), 100-104. https://doi.org/10.1111/j.1753-4887.2008.00145.x

Morris, R. T., Laye, M. J., Lees, S. J., Rector, R. S., Thyfault, J. P., & Booth, F. W. (2008). Exercise-induced attenuation of obesity, hyperinsulinemia, and skeletal muscle lipid peroxidation in the OLETF rat. *J Appl Physiol (1985)*, *104*(3), 708-715. https://doi.org/10.1152/japplphysiol.01034.2007

Muckenthaler, M. U., Rivella, S., Hentze, M. W., & Galy, B. (2017). A Red Carpet for Iron Metabolism. *cell*, *168*(3), 344-361. https://doi.org/10.1016/j.cell.2016.12.034

Murdolo, G., Bartolini, D., Tortoioli, C., Vermigli, C., Piroddi, M., & Galli, F. (2023). Accumulation of 4-Hydroxynonenal Characterizes Diabetic Fat and Modulates Adipogenic Differentiation of Adipose Precursor Cells. *International Journal of Molecular Sciences*, *24*(23), 16645.

Oliveira, A., & Vaz, C. (2015). The role of sarcopenia in the risk of osteoporotic hip fracture. *Clin Rheumatol*, *34*(10), 1673-1680. https://doi.org/10.1007/s10067-015-2943-9

Orr, J. S., Kennedy, A., Anderson-Baucum, E. K., Webb, C. D., Fordahl, S. C., Erikson, K. M., Zhang, Y., Etzerodt, A., Moestrup, S. K., & Hasty, A. H. (2014). Obesity alters adipose tissue macrophage iron content and tissue iron distribution. *Diabetes*, *63*(2), 421-432.

935 Ostler, J. E., Maurya, S. K., Dials, J., Roof, S. R., Devor, S. T., Ziolo, M. T., & Periasamy, M. (2014). Effects
936 of insulin resistance on skeletal muscle growth and exercise capacity in type 2 diabetic mouse
937 models. *American Journal of Physiology-Endocrinology and Metabolism*, *306*(6), E592-E605.
938 Paglialunga, S., Ludzki, A., Root-McCaig, J., & Holloway, G. P. (2015). In adipose tissue, increased
939 mitochondrial emission of reactive oxygen species is important for short-term high-fat
940 diet-induced insulin resistance in mice. *Diabetologia*, *58*(5), 1071-1080.
941 https://doi.org/10.1007/s00125-015-3531-x
942 Palstra, A. P., Beltran, S., Burgerhout, E., Brittijn, S. A., Magnoni, L. J., Henkel, C. V., Jansen, H. J., Van
943 Den Thillart, G. E., Spaink, H. P., & Planas, J. V. (2013). Deep RNA sequencing of the skeletal
944 muscle transcriptome in swimming fish. *PloS one*, *8*(1), e53171.
945 Park, M. W., Cha, H. W., Kim, J., Kim, J. H., Yang, H., Yoon, S., Boonpraman, N., Yi, S. S., Yoo, I. D., &
946 Moon, J.-S. (2021). NOX4 promotes ferroptosis of astrocytes by oxidative stress-induced lipid
947 peroxidation via the impairment of mitochondrial metabolism in Alzheimer's diseases. *Redox*
948 *biology*, *41*, 101947.
949 Pattanakuhar, S., Sutham, W., Sripetchwandee, J., Minta, W., Mantor, D., Palee, S., Pratchayasakul, W.,
950 Chattipakorn, N., & Chattipakorn, S. C. (2019). Combined exercise and calorie restriction
951 therapies restore contractile and mitochondrial functions in skeletal muscle of obese-insulin
952 resistant rats. *Nutrition*, *62*, 74-84. https://doi.org/10.1016/j.nut.2018.11.031
953 Pedersen, B. K., & Febbraio, M. A. (2008). Muscle as an endocrine organ: focus on muscle-derived
954 interleukin-6. *Physiol Rev*, *88*(4), 1379-1406. https://doi.org/10.1152/physrev.90100.2007
955 Pei, Z., Liu, Y., Liu, S., Jin, W., Luo, Y., Sun, M., Duan, Y., Ajoolabady, A., Sowers, J. R., & Fang, Y. (2021).
956 FUNDC1 insufficiency sensitizes high fat diet intake-induced cardiac remodeling and
957 contractile anomaly through ACSL4-mediated ferroptosis. *Metabolism*, *122*, 154840.
958 Pengam, M., Moisan, C., Simon, B., Guernec, A., Inizan, M., & Amérand, A. (2020). Training protocols
959 differently affect AMPK-PGC-1α signaling pathway and redox state in trout muscle. *Comp*
960 *Biochem Physiol A Mol Integr Physiol*, *243*, 110673.
961 https://doi.org/10.1016/j.cbpa.2020.110673
962 Ramana, K. V., Srivastava, S., & Singhal, S. S. (2014). Lipid peroxidation products in human health and
963 disease 2014. *Oxid Med Cell Longev*, *2014*, 162414. https://doi.org/10.1155/2014/162414
964 Rinnankoski-Tuikka, R., Silvennoinen, M., Torvinen, S., Hulmi, J. J., Lehti, M., Kivelä, R., Reunanen, H., &
965 Kainulainen, H. (2012). Effects of high-fat diet and physical activity on pyruvate
966 dehydrogenase kinase-4 in mouse skeletal muscle. *Nutrition & metabolism*, *9*, 1-13.
967 Rogers, P., & Webb, G. P. (1980). Estimation of body fat in normal and obese mice. *British Journal of*
968 *Nutrition*, *43*(1), 83-86.
969 Ruegsegger, G. N., & Booth, F. W. (2018). Health benefits of exercise. *Cold Spring Harbor perspectives*
970 *in medicine*, *8*(7), a029694.
971 Samuel, V. T., & Shulman, G. I. (2012). Mechanisms for insulin resistance: common threads and missing
972 links. *cell*, *148*(5), 852-871. https://doi.org/10.1016/j.cell.2012.02.017
973 Savira, M., Rusdiana, S. S. W., & Syahputra, M. (2020). Comparison Malondialdehyde (MDA) Level
974 between Obesity Non Metabolic Syndrome and Obesity with Metabolic Syndrome Patients.
975 *Age*, *53*(11.3), 44.55-10.48.
976 Shi, Y., Zhong, L., Liu, Y., Xu, S., Dai, J., Zhang, Y., & Hu, Y. (2024). Dietary sanguinarine supplementation
977 recovers the decrease in muscle quality and nutrient composition induced by high-fat diets of

grass carp (Ctenopharyngodon idella). *Animal Nutrition*, *17*, 208-219. https://doi.org/https://doi.org/10.1016/j.aninu.2024.04.001

Shortreed, K. E., Krause, M. P., Huang, J. H., Dhanani, D., Moradi, J., Ceddia, R. B., & Hawke, T. J. (2009). Muscle-specific adaptations, impaired oxidative capacity and maintenance of contractile function characterize diet-induced obese mouse skeletal muscle. *PloS one*, *4*(10), e7293.

Sriwijitkamol, A., Ivy, J. L., Christ-Roberts, C., DeFronzo, R. A., Mandarino, L. J., & Musi, N. (2006). LKB1-AMPK signaling in muscle from obese insulin-resistant Zucker rats and effects of training. *American Journal of Physiology-Endocrinology and Metabolism*, *290*(5), E925-E932.

Stockwell, B. R., Angeli, J. P. F., Bayir, H., Bush, A. I., Conrad, M., Dixon, S. J., Fulda, S., Gascón, S., Hatzios, S. K., & Kagan, V. E. (2017). Ferroptosis: a regulated cell death nexus linking metabolism, redox biology, and disease. *cell*, *171*(2), 273-285.

Stockwell, B. R., & Jiang, X. (2019). A physiological function for ferroptosis in tumor suppression by the immune system. *Cell Metabolism*, *30*(1), 14-15.

Stringer, C., Wang, T., Michaelos, M., & Pachitariu, M. (2021). Cellpose: a generalist algorithm for cellular segmentation. *Nature Methods*, *18*(1), 100-106. https://doi.org/10.1038/s41592-020-01018-x

Suga, T., Kinugawa, S., Takada, S., Kadoguchi, T., Fukushima, A., Homma, T., Masaki, Y., Furihata, T., Takahashi, M., & Sobirin, M. A. (2014). Combination of exercise training and diet restriction normalizes limited exercise capacity and impaired skeletal muscle function in diet-induced diabetic mice. *Endocrinology*, *155*(1), 68-80.

Tanaka, Y., Aleksunes, L. M., Yeager, R. L., Gyamfi, M. A., Esterly, N., Guo, G. L., & Klaassen, C. D. (2008). NF-E2-related factor 2 inhibits lipid accumulation and oxidative stress in mice fed a high-fat diet. *J Pharmacol Exp Ther*, *325*(2), 655-664. https://doi.org/10.1124/jpet.107.135822

Tang, D., Chen, X., Kang, R., & Kroemer, G. (2021). Ferroptosis: molecular mechanisms and health implications. *Cell Research*, *31*(2), 107-125. https://doi.org/10.1038/s41422-020-00441-1

Tsekoura, M., Kastrinis, A., Katsoulaki, M., Billis, E., & Gliatis, J. (2017). Sarcopenia and Its Impact on Quality of Life. *Adv Exp Med Biol*, *987*, 213-218. https://doi.org/10.1007/978-3-319-57379-3_19

Vellers, H. L., Letsinger, A. C., Walker, N. R., Granados, J. Z., & Lightfoot, J. T. (2017). High Fat High Sugar Diet Reduces Voluntary Wheel Running in Mice Independent of Sex Hormone Involvement. *Front Physiol*, *8*, 628. https://doi.org/10.3389/fphys.2017.00628

Walsh, M. E., Shi, Y., & Van Remmen, H. (2014). The effects of dietary restriction on oxidative stress in rodents. *Free Radical Biology and Medicine*, *66*, 88-99.

Wang, H., An, P., Xie, E., Wu, Q., Fang, X., Gao, H., Zhang, Z., Li, Y., Wang, X., & Zhang, J. (2017). Characterization of ferroptosis in murine models of hemochromatosis. *Hepatology*, *66*(2), 449-465.

Wang, H., Liu, C., Zhao, Y., & Gao, G. (2020). Mitochondria regulation in ferroptosis. *European journal of cell biology*, *99*(1), 151058.

Wang, Y., Zhang, Z., Jiao, W., Wang, Y., Wang, X., Zhao, Y., Fan, X., Tian, L., Li, X., & Mi, J. (2022). Ferroptosis and its role in skeletal muscle diseases. *Frontiers in molecular biosciences*, *9*, 1051866.

Weber, D., & Lanci, R. (2021). Lipid peroxidation and cancer. *Cancer Adv*, *4*(6), 24.

1020 Wei, S., Qiu, T., Yao, X., Wang, N., Jiang, L., Jia, X., Tao, Y., Wang, Z., Pei, P., & Zhang, J. (2020). Arsenic
1021 induces pancreatic dysfunction and ferroptosis via mitochondrial ROS-autophagy-lysosomal
1022 pathway. *Journal of hazardous materials*, *384*, 121390.
1023 Weisberg, S. P., McCann, D., Desai, M., Rosenbaum, M., Leibel, R. L., & Ferrante, A. W. (2003). Obesity
1024 is associated with macrophage accumulation in adipose tissue. *The Journal of clinical*
1025 *investigation*, *112*(12), 1796-1808.
1026 Welch, A. A., Hayhoe, R. P. G., & Cameron, D. (2020). The relationships between sarcopenic skeletal
1027 muscle loss during ageing and macronutrient metabolism, obesity and onset of diabetes.
1028 *Proc Nutr Soc*, *79*(1), 158-169. https://doi.org/10.1017/s0029665119001150
1029 Wenzel, S. E., Tyurina, Y. Y., Zhao, J., Croix, C. M. S., Dar, H. H., Mao, G., Tyurin, V. A., Anthonymuthu, T.
1030 S., Kapralov, A. A., & Amoscato, A. A. (2017). PEBP1 wardens ferroptosis by enabling
1031 lipoxygenase generation of lipid death signals. *cell*, *171*(3), 628-641. e626.
1032 Wesolowski, L. T., Semanchik, P. L., & White-Springer, S. H. (2022). Beyond antioxidants: Selenium and
1033 skeletal muscle mitochondria. *Front Vet Sci*, *9*, 1011159.
1034 https://doi.org/10.3389/fvets.2022.1011159
1035 Wilkinson, D. J., Hossain, T., Hill, D. S., Phillips, B. E., Crossland, H., Williams, J., Loughna, P.,
1036 Churchward-Venne, T. A., Breen, L., Phillips, S. M., Etheridge, T., Rathmacher, J. A., Smith, K.,
1037 Szewczyk, N. J., & Atherton, P. J. (2013). Effects of leucine and its metabolite
1038 β-hydroxy-β-methylbutyrate on human skeletal muscle protein metabolism. *J Physiol*, *591*(11),
1039 2911-2923. https://doi.org/10.1113/jphysiol.2013.253203
1040 Xiang, Y.-Y., Baek, K.-W., Won, J.-H., Park, Y., Kim, J.-S., Xiang, Y.-Y., Baek, K.-W., Won, J.-H., Park, Y., &
1041 Kim, J.-S. (2023). Effects of Lifelong Aerobic Exercise on Ferroptosis-Related Gene Expressions
1042 in Kidney of Aged Mice. *Exercise Science*, *32*(4), 410-418.
1043 Xiao, R., Wei, Y., Zhang, Y., Xu, F., Ma, C., Gong, Q., Gao, J., & Xu, Y. (2022). Trilobatin, a Naturally
1044 Occurring Food Additive, Ameliorates Exhaustive Exercise-Induced Fatigue in Mice:
1045 Involvement of Nrf2/ARE/Ferroptosis Signaling Pathway. *Front Pharmacol*, *13*, 913367.
1046 https://doi.org/10.3389/fphar.2022.913367
1047 Yang, W. S., SriRamaratnam, R., Welsch, M. E., Shimada, K., Skouta, R., Viswanathan, V. S., Cheah, J. H.,
1048 Clemons, P. A., Shamji, A. F., & Clish, C. B. (2014). Regulation of ferroptotic cancer cell death
1049 by GPX4. *cell*, *156*(1), 317-331.
1050 Yang, Y., Smith, D. L., Jr., Keating, K. D., Allison, D. B., & Nagy, T. R. (2014). Variations in body weight,
1051 food intake and body composition after long-term high-fat diet feeding in C57BL/6J mice.
1052 *Obesity (Silver Spring)*, *22*(10), 2147-2155. https://doi.org/10.1002/oby.20811
1053 Yang, Y., Smith Jr, D. L., Keating, K. D., Allison, D. B., & Nagy, T. R. (2014). Variations in body weight,
1054 food intake and body composition after long-term high-fat diet feeding in C57BL/6J mice.
1055 *Obesity*, *22*(10), 2147-2155.
1056 Yeu, J., Ko, H. J., Kim, D., Ahn, Y., Kim, J., Lee, W., Jung, I., Suh, J., & Lee, S. J. (2019). Evaluation of
1057 iNSiGHT VET DXA (Dual-Energy X-ray Absorptiometry) for assessing body composition in
1058 obese rats fed with high fat diet: a follow-up study of diet induced obesity model for 8 weeks.
1059 *Lab Anim Res*, *35*, 2. https://doi.org/10.1186/s42826-019-0004-2
1060 Yu, Y., Jiang, L., Wang, H., Shen, Z., Cheng, Q., Zhang, P., Wang, J., Wu, Q., Fang, X., & Duan, L. (2020).
1061 Hepatic transferrin plays a role in systemic iron homeostasis and liver ferroptosis. *Blood, The*
1062 *Journal of the American Society of Hematology*, *136*(6), 726-739.

1063 Zhang, X., Ma, Y., Lv, G., & Wang, H. (2023). Ferroptosis as a therapeutic target for
1064 inflammation-related intestinal diseases. *Front Pharmacol*, *14*, 1095366.
1065 https://doi.org/10.3389/fphar.2023.1095366
1066 Zhang, Y., Fischer, K. E., Soto, V., Liu, Y., Sosnowska, D., Richardson, A., & Salmon, A. B. (2015).
1067 Obesity-induced oxidative stress, accelerated functional decline with age and increased
1068 mortality in mice. *Archives of biochemistry and biophysics*, *576*, 39-48.
1069 Zhao, X., Si, L., Bian, J., Pan, C., Guo, W., Qin, P., Zhu, W., Xia, Y., Zhang, Q., & Wei, K. (2022). Adipose
1070 tissue macrophage-derived exosomes induce ferroptosis via glutathione synthesis inhibition
1071 by targeting SLC7A11 in obesity-induced cardiac injury. *Free Radical Biology and Medicine*,
1072 *182*, 232-245.
1073 Zhuang, A., Yang, C., Liu, Y., Tan, Y., Bond, S. T., Walker, S., Sikora, T., Laskowski, A., Sharma, A., de Haan,
1074 J. B., Meikle, P. J., Shimizu, T., Coughlan, M. T., Calkin, A. C., & Drew, B. G. (2021). SOD2 in
1075 skeletal muscle: New insights from an inducible deletion model. *Redox Biol*, *47*, 102135.
1076 https://doi.org/10.1016/j.redox.2021.102135
1077 Zimmermann, M. B., & Hurrell, R. F. (2007). Nutritional iron deficiency. *Lancet*, *370*(9586), 511-520.
1078 https://doi.org/10.1016/s0140-6736(07)61235-5